ARTIFICIAL NEURAL NETWORK BASED TOOL FOR BUCKLING LOADS OF INTEGRALLY STIFFENED AIRCRAFT STRUCTURAL PANELS

A THESIS SUBMITTED TO
THE GRADUATE SCHOOL OF NATURAL AND APPLIED SCIENCES
OF
MIDDLE EAST TECHNICAL UNIVERSITY

BY

SELÇUK GÜZEL

IN PARTIAL FULFILLMENT OF THE REQUIREMENTS
FOR
THE DEGREE OF MASTER OF SCIENCE
IN
AEROSPACE ENGINEERING

FEBRUARY 2021

Approval of the thesis:

ARTIFICIAL NEURAL NETWORK BASED TOOL FOR BUCKLING LOADS OF INTEGRALLY STIFFENED AIRCRAFT STRUCTURAL PANELS

submitted by **SELÇUK GÜZEL** in partial fulfillment of the requirements for the degree of **Master of Science** i**n Aerospace Engineering, Middle East Technical University** by,

Prof. Dr. Halil Kalıpçılar
Director, Graduate School of **Natural and Applied Sciences** _____

Prof. Dr. İsmail Hakkı Tuncer
Head of the Department, **Aerospace Engineering** _____

Assoc. Prof. Dr. Ercan Gürses
Supervisor, **Aerospace Engineering** _____

Examining Committee Members:

Prof. Dr. Altan Kayran
Aerospace Engineering, METU _____

Prof. Dr. Demirkan Çöker
Aerospace Engineering, METU _____

Prof. Dr. Erdem Acar
Mechanical Engineering, TOBB University of Economics and Technology _____

Assoc. Prof. Dr. Ercan Gürses
Aerospace Engineering, METU _____

Assoc. Prof. Dr. Tuncay Yalçınkaya
Aerospace Engineering, METU _____

Date: 15.02.2021

I hereby declare that all information in this document has been obtained and presented in accordance with academic rules and ethical conduct. I also declare that, as required by these rules and conduct, I have fully cited and referenced all material and results that are not original to this work.

Name, Last name : Selçuk Güzel

Signature :

ABSTRACT

ARTIFICIAL NEURAL NETWORK BASED TOOL FOR BUCKLING LOADS OF INTEGRALLY STIFFENED AIRCRAFT STRUCTURAL PANELS

Güzel, Selçuk
Master of Science, Aerospace Engineering
Supervisor: Assoc. Prof. Dr. Ercan Gürses

February 2021, 88 pages

The sudden change in the load carrying capacity under compresive loading, called buckling, may cause catastrophic failures. Therefore, determination of the first buckling and collapse loads of structural elements is essential in preliminary design stages. Finite element (FE) analyses and structural testing are used to determine buckling characteristics of a structural element. However, in early design stages, FE analyses are time consuming and structural testing is costly. In this study, an artificial neural network tool (ANN) is used to reduce computational effort to determine buckling loads of integrally stiffened structural panels in early design stages. Reuslts of FE analyses are employed to train the ANN. Moreover, Latin Hypercube Sampling (LHS) methodology is used to reduce the number of required FE analyses to generate database that artificial neural network is based on. Finally, a Multi-fidelity sampling algorithm that uses FE models with different mesh resolutions is implemented for generation of the ANN database in order to reduce computational time spent for finite element analyses. Mean errors and fit performance model results are compared to determine accuracy of the neural network results.

Keywords: Structural Optimization, Artificial Neural Network, Integrally Stiffened Structures, Multi Fidelity Sampling Algorithm, Latin Hypercube Sampling.

ÖZ

ENTEGRE GÜÇLENDİRİLMİŞ YAPISAL PANELLER İÇİN YAPAY SİNİR AĞI BAZLI BURKULMA YÜKLERİ BELİRLEME ARACI

Güzel, Selçuk
Yüksek Lisans, Havacılık ve Uzay Mühendisliği
Tez Yöneticisi: Doç. Dr. Ercan Gürses

Şubat 2021, 88 sayfa

Basma yükeri altında yapısal parçalarda yük taşıma kapasitesindeki ani düşüş, diğer adıyla burkulma uçak yapısallarında geri dönüşü olmayan hasarlara sebep olur. Bu sebeple ön tasarım süreçlerinde tasarlanan parçaların burkluma ve çökme yüklerinin tespit edilmesi hayati önem arzetmektedir. Bu yükleri tespit etmede ticari sonlu eleman yazılımları ve yapısal testlerden yararlanılmaktadır. Ancak ön tasarım süreçleri için yapısal analizler zaman kaybına sebep olurken yapısal testler de maliyetlidir. Bu çalışmada, ön tasarım süreçlerinde kaybedilen zamanı azaltmak amacıyla, entegre güçlendirilmiş yapısal paneller için yapay sinir ağı bazlı ilk burkulma ve çökme yükleri belirleme yöntemi geliştirilmesi hedeflenmiştir. Sonlu eleman analizleri yapay sinir ağlarını eğitmek için kullanılmıştır. Ayrıca *Latin Hiperküp Örnekleme Metodolojisi* ile yapay sinir ağı data havuzunu oluşturmak için gerekli sonlu eleman analiz sayısının azaltılması amaçlanmıştır. Son olarak *Değişken Doğruluk Seviyeli Seçim Algoritmalarıyla* yapay sinir ağı data havuzu için harcanan süreyi azaltmak amaçlanmıştır. Oluşturulan yöntemden alınan sonuçlar ortalama hata kıyaslamalarıyla değerlendirilmiştir.

Anahtar Kelimeler: Yapısal Optimizasyon, Yapay Sinir Ağı, Entegre Güçlendirilmiş Paneller, Değişken Doğruluk Seviyeli Seçim Algoritmaları, Latin Hiperküp Örnekleme Metodolojisi.

To My Family…

ACKNOWLEDGMENTS

Firstly, I would like to express my sincere gratitude to my supervisor Assoc. Prof. Dr. Ercan Gürses for his advice, guidance, and recommendations throughout the study.

Besides my advisor, I would like to thank the rest of my thesis committee: Prof. Dr. Altan Kayran, Prof. Dr. Demirkan Çöker, Prof. Dr. Erdem Acar, and Assoc. Prof. Dr. Tuncay Yalçınkaya, for their insightful comments and contributions.

I would like to thank to my chief engineers Dr. Orhan Gülcan, Bilge Aziz Çoğuz and Erhan Çiftçi for their guidance, motivation, and support against every major problem that I face with throughout the preparation of this study. Also, I would like to thank to my colleague Büşra Bartan Kumbasar for sharing her experiences about finite element analysis.

Finally, I must express my very profound gratitude to my parents Yusuf and Funda Güzel, to my brother Emre Güzel for providing me an unfailing support and continuous encouragement throughout the process of this study.

TABLE OF CONTENTS

LIST OF TABLES

TABLES

LIST OF FIGURES

FIGURES

CHAPTERS

CHAPTER 1

INTRODUCTION

Determination of load carrying capacities of aircraft structures is the major problem in the preliminary stages of the aircraft design. Aircraft structures give different responses and show different failure characteristics against different loading conditions. Therefore, each structural element has to be investigated under each loading type. This investigation can be done by finite element analysis (FEA) and structural testing. However, structural testing is costly and FE analyses are time consuming especially in preliminary design stages when everything can be changed in a short period of time and reaching the optimum structural design for a given load case becomes challenging.

Buckling is a structural instability in which load carrying capacity of a structural element may suddenly decrease. This sudden change can cause catastrophic failures meaning that it can cause structural component to fail completely which can lead to lose of the aircraft. Therefore, determination of buckling and collapse loads of the structure is essential especially in preliminary design stages. To achieve this goal, commercial finite element analysis tools are used generally in the aerospace industry.

FEA requires a finite element model that is used to implement the load and boundary conditions, configuration of the analysis parameters, and calculation of the desired outputs. The time spent for the analysis increases significantly depending on the complexity of the structure. Depending on the situation, geometrical details, material behavior, type of loading and boundary conditions can be hard to solve numerically. Moreover, nonlinear material behavior and geometric nonlinearities can increase the time spent for FEA significantly. In addition, many repetitions of finite element analyses and update of models during the optimization process can increase the

computational time further since FEA gives reasonable and realistic results if and only if implementation of boundary conditions and generation of finite element model reflects the reality.

In this study, it is aimed to reduce time spent for finite element analyses to reach the optimum integrally stiffened structural panel design. The *Artificial Neural Network* tool is used to determine the first buckling and collapse loads of the integrally stiffened structural panels. ANN is a computation tool that can classify and recognize patterns and provide accurate prediction for the given inputs by learning from the past [1]. The first in-plane load level that the load carrying capacity suddenly drops is called *the first buckling load* and the loading level that structure completely loses the load carrying ability meaning that structure fails is called *the collapse load*.

The ANN tool requires a database to be trained and to determine buckling characteristics of the target design points. This database is generated via FEA results. Finite element analyses are performed in commercial finite element analysis program *ABAQUS* and the ANN tool is generated via *nntoolbox* of *MATLAB* software. Then, the ANN is used to predict *the first buckling load*, *the collapse load* and *the mass* of integrally stiffened structural panels.

In this study, finite element analysis procedure is explained in Chapter 2 and Chapter 3. The generation and training processes of the ANN are described in Chapter 4. In Chapter 5 the performance parameters and results obtained by FEA and ANN tool are compared to verify the ANN tool. Finally, conclusions and possible future works are described in Chapter 6.

CHAPTER 2

LITERATURE REVIEW

The present method of designing and building primary airliner structures is called semi-monocoque, such as fuselages. There are thousands of detail parts riveted to transverse stiffeners or ribs and to longitudinal stiffeners or ribs in the semi-monocoque structure, all of which are riveted to the skin. It is possible to provide more efficient structures that are less labor intensive, costly, and time-consuming to design, fabricate and assemble, although semi-monocoque structures are successful for their operational purpose. Moreover, for a major airliner, many manufacturing shops are usually used to produce the various parts of a semi-monocoque design. Indeed, there are about three million holes drilled into parts with an equal number of fasteners mounted in a commercial jetliner, all of which are performed and coordinated by over one thousand manufacturing shops [2].

For almost all fuselage cracks, fastener holes are the source or origination position, which appear to decrease the airframe's service life. In addition, it is also recognized that fastener holes are the main culprit in the creation of multi-site fatigue damage, corrosion fretting, and expensive inspection, refurbishment, and maintenance of aircraft. Less time is required to perform regular inspections and repair fastener holes to ensure the airliner's structural integrity with less fastener holes [2].

Therefore, in order to overcome construction and maintenance problems of the semi-monocoque structures, integrally stiffened structural panels are proposed. By using integrally stiffened panels, which are numerically controled machined parts, stringers and frames are assembled to the structure without any rivet which increases strucutural integrity. Moreover, the application reduces the cost and labor-intensity of the products.

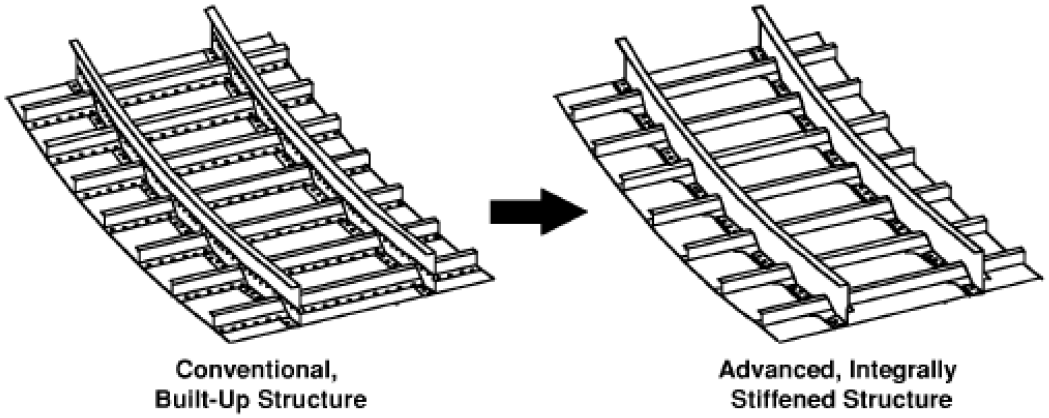

Figure 2.1. Built-Up vs Integrally Stiffened Structural Panels [3]

The buckling is one of the failure modes of the structure which cause a sudden load carriying capacity change. In a study conducted by Alinia et al. [4] an unstiffened panel was investigated from start of the loading until the failure. It was observed that buckling occurs after a critical loading point. This critical load depends on elastic material properties and geometry of the panel according to the study.

Parameters that effect buckling characteristics of structural panels have been investigated by several works in literature. These parameters were investigated by numerical simulations in Chong and Ramm [5]. Initial conditions affecting buckling have been investigated and the structural response of the structure has been studied under buckling and post-buckling. In order to show that the simulations are useful for obtaining the structural properties of a structural plate, numerical simulations and test results were compared. In the study of Ferreira and Virtuoso [6], two semi-analytical methods were developed and used to conduct a nonlinear stability analysis of structural panels. It was seen that the boundary conditions affect the buckling characteristics of the structure significantly. Muameleci[7] performed a study using two separate commercial finite element programs, ABAQUS and NASTRAN, contrasting simple-supported and clamped edge conditions. Geometric properties and boundary conditions have been shown to have major effects on buckling characteristics. The research performed in this study was also checked by the results of the test and contrasted with conventional methodologies of structural analysis. In

the study of Amani et al., the effects of nonlinear material properties, geometric properties, and initial imperfections on buckling and post-buckling behaviour were studied [8]. A study of conventional methods and the Finite Element System (FEM) for elastic buckling was also carried out. In addition, a comparative analysis was carried out in the Aydın [9] study to determine the post-buckling load distribution of structural panels with and without material nonlinearity.

In order to validate a method with FEM, it is important to use the FEM with maximum care. In order to obtain precise results from the FEA, several experiments have been carried out on the finite element modeling of stiffened panels. In the study conducted by Lynch et al. [10], guidelines were proposed as the element selection, the mesh consistency, the skin-stringer connection idealization, the initial conditions, and the solution procedures to determine the ultimate load carrying ability of skin-stringer assemblies. The key aspects of finite element modeling for stiffened panels operating under compression loads have been established. Guidelines were developed in a similar way for the skin-stringer assemblies operating under shear loads in the analysis of Murphy et al.[11]. By observing the effects of model parameters, Campbell et al.[12] focused on idealization errors produced during the FEA procedure and monitoring these errors. The findings showed that a crucial parameter for the determination of the buckling load is the modeling of boundary conditions. Also, the material model and idealization of the geometry of stiffeners influence the ultimate strength measurement of a stiffened panel. In the study of Wang [13], nonlinear finite element studies were carried out with different solution procedures in order to study the parameters influencing the behavior of buckling and post-buckling. The material model, the geometric properties, and the boundary conditions of the structure have been found to be those parameters. To validate the FEA, the findings were compared with test results.

It takes several trials to design an optimum aircraft structure before an optimum design is achieved. Therefore, by minimizing the number of experiments, the time required for the design must be reduced. Several techniques have been developed and used for stiffened panels to minimize the number of trials. An intelligent

optimization framework is used in the study of Hao [14] to increase the optimization performance of the curvilinearly stiffened structural panels. In Bisagni and Lanzi [15], by adding an Artificial Neural Network (ANN) tool that is developed for weight reduction of a stiffened panel, it was intended to decrease analysis time. The tool offers a skin-stringer assembly with an optimum load carrying capacity and weight. Artificial neural networks are tools of pattern recognition and classification and the origin of the ANN is the neural structure of central nervous system and in literature it is commonly used for structural design and optimization purposes. As an example, ANN was used for optimization purposes in a compression member optimization study conducted by Sheidaii and Bahraminejad [16]. In the analysis, the load-displacement relationship was obtained using analytical methods for different types of columns. To shape a data set to train an ANN, the findings were used. In the study of Cankur [17], an artificial neural network-based analysis tool was developed for traditional skin-stringer structures and used under uni-axial compression to evaluate the mass, buckling and collapse loads of skin-stringer structures. Also, in a study conducted by Yıldırım [18] [19], based on ANN, a bolted flange design tool was made. With finite element model parameters and corresponding results of analysis, a data set was developed. The data set was used in ANN's training. FEA and methodological approaches were contrasted with the ANN findings. Comparisons have shown that the ANN findings are reliable to be used in the design of bolted flanges. Optimization studies are not only for metallic structures but also composite structures as well. According to the study conducted on anisotropic laminated composites [20], to optimize the construction of a laminated composite, a generic algorithm and two ANNs are used. It was concluded that the use of these techniques leads to sufficiently specific solutions and decreases the time needed for the design process. Lastly, in the study of Okul [21], for traditional skin-stringer structures, an artificial neural network-based analysis tool is generated and used to evaluate the mass, buckling and collapse loads of the skin-stringer structures under combined compression and shear loads. These studies are clear examples of the suitability of the ANN as an instrument in the design and study of aircraft structures.

ANN based tools have also been used to determine buckling and collapse loads of structural panels. By producing an ANN as a function of initial imperfections, Sadovsky and Soares[22] obtained post-buckling strength of a thin rectangular plate. To provide fair collapse load outcomes, the generated ANN is accurate enough. In a study by Lanzi and Giavotto [23], ANN was used for post-buckling optimization for stiffened panels. In this analysis, various optimization methods, including ANN, were used to optimize composite stiffened panels subjected to axial compression. Tests have confirmed the findings and it has been concluded that both the buckling load and the collapse load can be fairly determined. The Mallela and Upadhyay[24] also focussed on the prediction of buckling loads for composite stiffened panels operating under shear loads. In a database for the training of an ANN instrument, FEA results for various composite structures were gathered. An effective tool for optimization purposes was developed in this study.

The generation of ANN database is quite critical procedure since it takes too much time. One has to chose a smart way to generate the ANN database in order to reduce the time spent. There are different design of experiment methodologies in literature to select experimental data in a strategic way. One the methodologies is called *Latin Hypercube Sampling (LHS)* which is explained in Section 4.2.2 and it is commonly used in structural engineering. In the study of Olsson et al. [25], LHS was used to improve computational efficiency of the stochastic finite element analysis. Moreover, in the study of Ding et al. [26], LHS was used to calculate accurate fracture probability. The number of simulations were relatively small and the calculation error was satisfactory in the study. Moreover, in the study of Ferrari et al. [27], the LHS was employed to select experimental vibration data in order to boost the confidence degree of the develeped model for a concrete bridge. According to the results of the study, there was a good match between results taken from experiments and finite element analysis. Therefore, it can be stated from the studies above that the LHS is quite effective tool to increase computational efficiency and to reduce the time required to generate a database.

Another way to generate the ANN database efficiently is the *Multi-Fidelity Sampling* and it is recently becomming a useful technique to improve computational efficiency in several engineering applications. In the study of Huang [28], in order not to train a full database with high-fidelity models since they are time consuming, multi-fidelity sampling was applied for a systems engineering problem. In order to accurately compare all design alternatives, the proposed framework uses low-fidelity models and then assigns a fixed budget of high-fidelity models to look for the best design based on low-fidelity simulation performance. Another study was performed by Böhnke et al. [29]. In this study, a design environment is implemented consisting of a structure, a core model and a newly developed conceptual design module for aircraft. The aerodynamics, primary structures, mission analysis and climate impact modules were already using a high-fidelity analysis tools. However, in order to improve the capabilities of the tools, there is a need to merge the database and they uitlize the multi-fidelity sampling in this study. In the study of Yoo et al. [30], A probabilistic optimization framework for composite structures based on multi-fidelity modeling has been introduced. The established multi-fidelity formulation dramatically reduces the computational time needed, enabling more design variables to be considered early in the design process. The results showed that multi-fidelity models provide high levels of accuracy while reducing computation time drastically. Therefore, the multi-fidelity sampling is a useful methodology to preserve the solution accuracy with significant reduction in computation time.

In this study, an ANN based computation tool is created to determine the mass, first buckling load and the collapse load of the integrally stiffened structural panels under uni-axial compression. Moreover, in order to reduce computational time spent for the generation of ANN database, the LHS and the multi-fidelity sampling algorithm are employed. Finally, the databases generated are investigated in terms of accuracy and computational time.

CHAPTER 3

BUCKLING ANALYSIS OF INTEGRALLY STIFFENED PANELS

In order to obtain accurate results in finite element analyses (FEA) of structural parts and assemblies, significant computational power and time are required. Especially, nonlinearity in geometry and material properties and finite element sizes are the major factors that increase the computational time.

In this study, it is aimed to create an Artificial Neural Network (ANN) based tool to determine first buckling and collapse loads of integrally stiffened panels and therefore reduce the time spent for the finite element analyses. To reach accurate results from ANN, 729 different finite element models are created, and 2187 finite element analyses are performed individually for three different element sizes. Database quality is vital in training of an ANN. Therefore, a convergence study is conducted to determine optimum element size for analyses. Moreover, different design of experiment methodologies are studied to reduce the number of analyses to create an ideal database and increase the performance of ANN.

A commercial finite element software ABAQUS is used in this study. The integrally stiffened panels are modeled as 2D shell elements. Then elastic and plastic material properties and density are given to the model with proper cross-sectional dimensions. Afterwards, parts are meshed by using 2D-quadrilateral elements and clamped boundary conditions are given to observe the buckling characteristics. The finite element model creation is performed individually to all models in database.

3.1 Geometry and Database Description

The first step of a finite element analysis is to generate the appropriate geometric model of the structure. Integrally stiffened panels generally consist of blade type stiffeners since the part itself is produced by numerically controlled (NC) machining.

A sample integrally stiffened panel drawing is given in Figure 3.1 and two-dimensional plan and cross-sectional views are given in Figure 3.2.

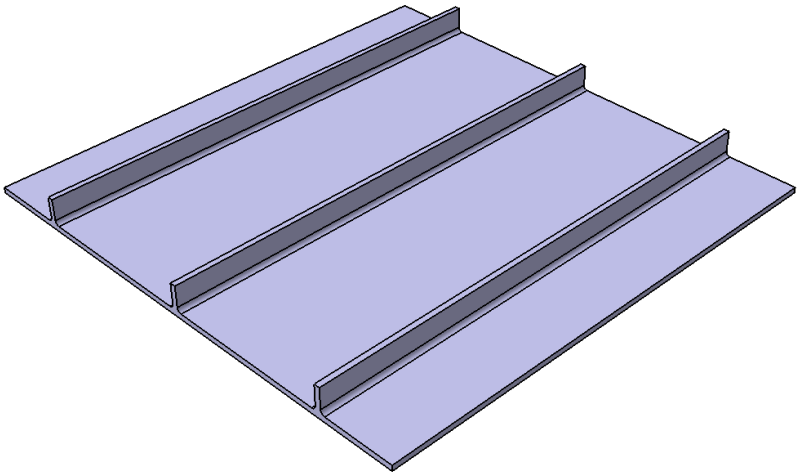

Figure 3.1. Design Model of a Sample Integrally Stiffened Panel

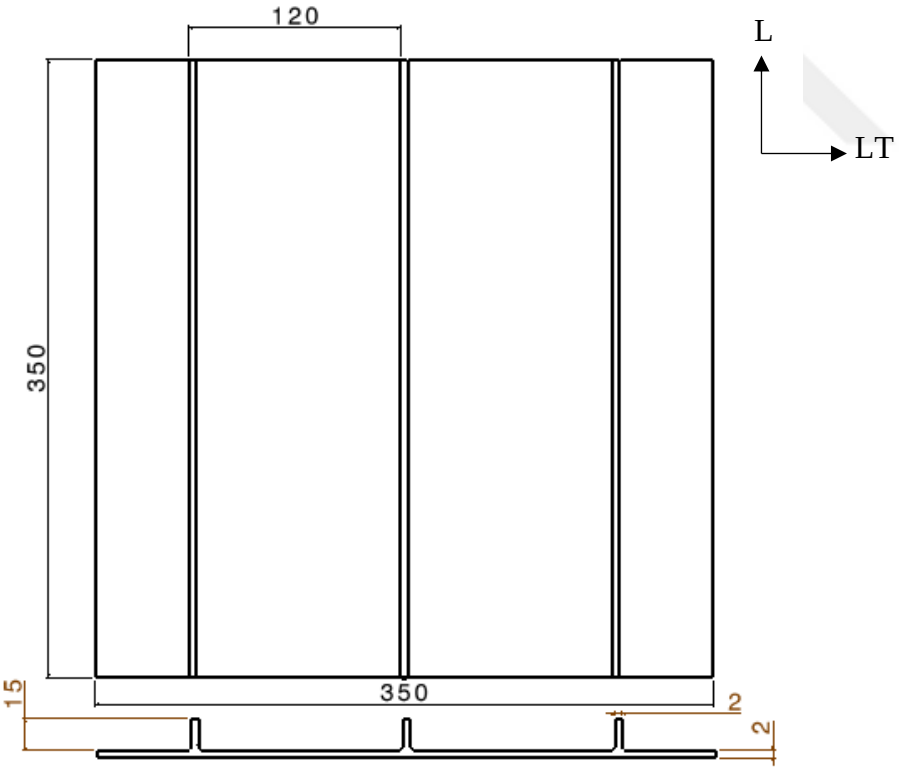

Figure 3.2. Technical Drawing of an Integrally Stiffened Panel

In Figure 3.2, “L” stands for material longitudinal direction and “LT” stands for material longitudinal transverse direction. There are six main parameters which affect the buckling response of a structure. Those are the length, the width, the stringer height, the stringer thickness, the skin thickness and the number of stringers. In this study, three levels of these parameters are determined, and all possible geometric combinations of them are modeled and analyzed. Dimensions of the panels are chosen as common aircraft design values, and they are given in Table 3.1.

Table 3.1 Geometric Dimensions of Integrally Stiffened Panels

PANEL DIMENSIONS	
LENGTH (mm)	350, 400, 450
WIDTH (mm)	350, 400, 450
STRINGER HEIGHT (mm)	15, 20, 25
STRINGER THICKNESS (mm)	1.5, 1.75, 2.0
SKIN THICKNESS (mm)	1.5, 1.75, 2.0
NUMBER OF STRINGERS	3, 4, 5

The schematic view of the finite element model of an integrally stiffened panel is given in Figure 3.3. A compressive load is applied to the panel in a displacement-controlled manner to avoid convergence problems. Two reference points, RP1RP3 in Figure 3.3, are created as master nodes of the integrally stiffened panel and used in boundary condition applications. The tie constraints are applied between the master node and slave nodes since ABAQUS defines tie constraints as connections of closest nodes on different surfaces, which equalize all active degrees of freedom [31]. RP1 is used as the load application point, and RP2 is used as the reaction point. Moreover, the reference point “RP3 is used as the master node of side nodes since, in aircraft structures, structural panels are constraint from all edges, and the analyses must simulate the aircraft structural application.

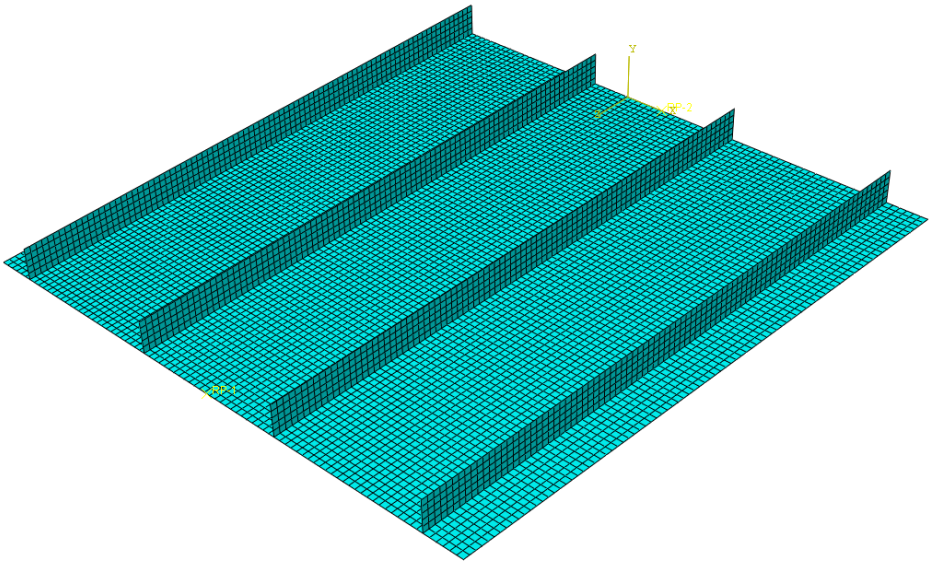

Figure 3.3. Finite Element Model of Integrally Stiffened Panel

3.2 Material Properties

A homogeneous shell section of aluminum 7050-T7451 is created and assigned to the FE model. Aluminum 7050 is a 7000 series aluminum alloy, and it is less quench sensitive, which gives the alloy to maintain strength properties over time, especially in thick sections. Tempering T7451 also provides better corrosion resistance, exfoliation resistance, and toughness. Therefore, aluminum 7050-T7451 is a commonly used material for numerically machined parts used for bulkheads, fuselages, or wing skins in the aerospace industry [32]. Material properties of aluminum 7050-T7451 are listed as follows [32]:

- ✓ Young's Modulus (E_c): 73084 MPa
- ✓ Poisson's Ratio (υ): 0.33
- ✓ Density (ρ): 2.83 g/cm^3
- ✓ Yield Strength (σ_0): 434.37 MPa
- ✓ Ramberg-Osgood Number (n): 15

More details about Aluminum 7050-T7451 are given in Appendix A. The uniaxial response of isotropic elastoplastic materials is described by the so-called "Ramberg-Osgood Equation" [33].

$$\epsilon = \frac{\sigma}{E} + 0.002\left(\frac{\sigma}{\sigma_0}\right)^n \tag{3.1}$$

In (3.1), ϵ is the uniaxial strain, σ is the uniaxial stress, E is the elastic modulus, σ_0 is the yield strength, and n is the Ramberg-Osgood number. (3.1) is used to generate the plastic material response of aluminum 7050-T7451 in this study.

Isotropic hardening plasticity of ABAQUS is used in the material definition without a hardening parameter to obtain an unloading curve parallel to the elastic loading curve.

In the definition of material properties in ABAQUS, with elastic properties of the material, true stress and corresponding true strain data are required to simulate the material's plastic response. The engineering plastic stress-strain data is generated by using (3.1) and converted to true stress-strain data with the help of (3.2) and (3.3).

$$\sigma_{tr} = \sigma_{eng}(1 + \epsilon_{eng}) \tag{3.2}$$

$$\epsilon_{tr} = \ln\left(1 + \epsilon_{eng}\right) \tag{3.3}$$

3.3 Mesh Quality

All models that are used for the generation of the database are modeled as shell elements. S4 type is assigned to the shell elements, a 4-node element with four integration points (full integration), having hourglass control, and finite membrane strains. ABAQUS recommends the S4 element in the modeling of the general purpose of shells. S4 elements use the discrete Kirchhoff thin shell theory for thin shells, and for thick shells, the thick shell theory is used [34]. As mentioned in ABAQUS documentation, the theory to be used is determined according to the element's thickness in calculations with S4 elements. Also, during the calculations, the changes in the thickness may cause the selected theory to change [31].

A mesh convergence study is conducted to determine the optimum mesh size for the analyses. Nine models are created with different mesh sizes and compared through the first buckling and the collapse loads of integrally stiffened panels. In the mesh convergence study, mesh sizes are selected as 4mm, 5mm, 6mm, 7mm, 8mm, 9mm, 10mm, 15mm, 20mm. The models are solved, and first buckling and collapse loads are obtained from the results. Table 3.2 shows both the first buckling and the collapse loads for each mesh size.

Table 3.2 First Buckling and Collapse Load Results for Different Mesh Sizes

Element Edge Size [mm]	First Buckling Load [kN]	Collapse Load [kN]
4	58.8	146.4
5	59.0	146.5
6	59.2	146.7
7	59.3	147.2
8	59.4	147.4
9	59.0	146.5
10	59.9	147.8
15	60.9	142.1
20	61.3	143.4

Table 3.2 shows that mesh sizes from 4mm up to 6mm give almost equal results both in buckling and collapse loads. For mesh sizes greater than 6 mm, the results show more discrepancies. The mesh sizes 15mm and 20mm give noticeable low collapse loads and appreciable high first buckling loads compared to the results taken from 4mm.

The force-displacement curves of the analyses are given in Figure 3.4 for the finest five mesh sizes.

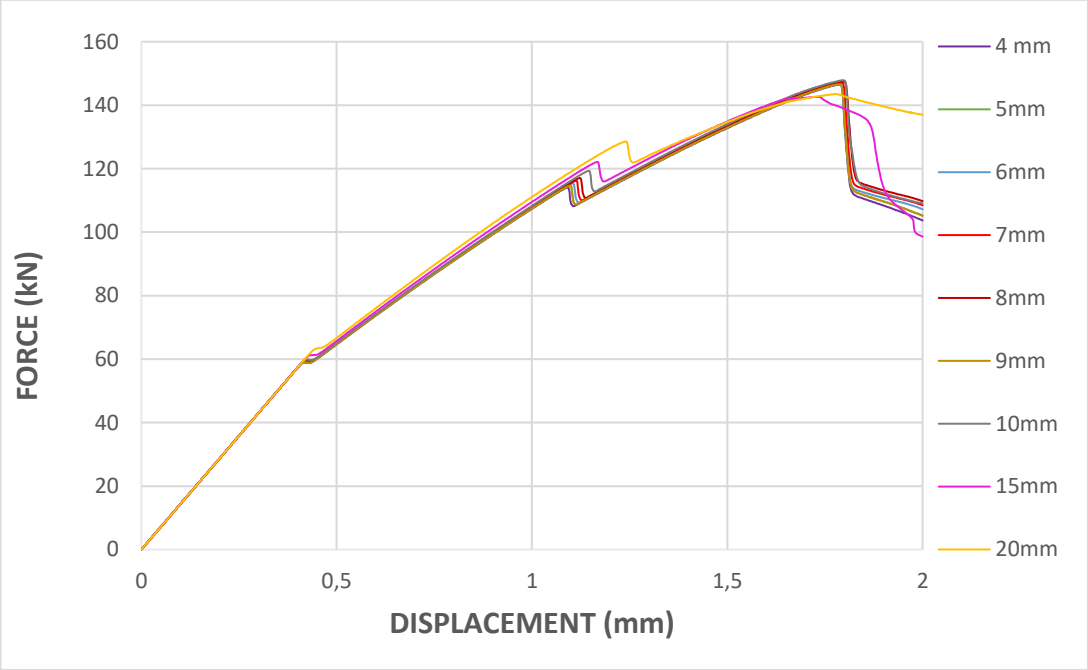

Figure 3.4. Force-Displacement Curves of the Models of Mesh Convergence Study

The models with 6 mm or smaller element size give remarkably close load-displacement curves, first buckling and collapse loads. Therefore, the mesh size is chosen as 5 mm for this study. Moreover, for multi-fidelity sampling study described in Chapter 4.2.3, the mid-quality mesh size is 10 mm, and the coarse mesh size is chosen as 20 mm.

The deformed meshes corresponding to the first buckling mode are shown in Figure 3.5 for the finest and the coarsest discretization.

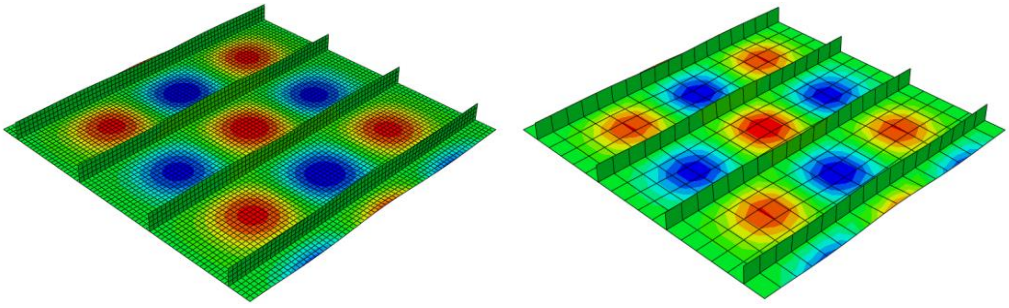

Figure 3.5. First Buckling Patterns of the Models with 5mm and 20mm Mesh Sizes

3.4 Finite Element Solution Methodology

In order to solve the buckling characteristics of the stiffened panels, *Static, General* step of the ABAQUS is utilized. The *Static, General* step uses Newton's method to solve nonlinear problems. Displacement controlled loading is given to the structure to avoid potential divergence problems during the solution procedure. Structural local and global instabilities occur during the solution because of the geometrical nature of the buckling. Numerical stabilization procedures must be applied to overcome local instabilities during the solution. In the *Static, General* solution step, an adaptive automatic stabilization option, which creates artificial damping leading to dissipation of a part of released strain energy, is used to increase the convergence of the solver. If the damping rate is too high, the solution accuracy may be low [31]. Therefore, tolerance values are defined to control the created damping and released strain energy. Dissipated energy fraction is specified as 0.0002, and the maximum ratio of stabilization energy to strain energy is defined as 0.05 as ABAQUS defaults. Moreover, *nlgeom* option is enabled to model nonlinear geometric effects properly. Also, the step size is chosen as a maximum of 0.001 seconds and a minimum of 1.0×10^{-7} seconds.

After defining the solution step, mass data, reaction forces and displacement data of corresponding reference points are requested as history outputs. Finally, the finite element solution methodology definition is completed, and the analysis is run with the parameters specified in this section.

3.5 Finite Element Analysis Results

The aim of the analysis is to determine the mass, the first buckling load, and the collapse load of the integrally stiffened structural panels. To this end load-displacement curves are obtained from the analyses. In Figure 3.6, an example load-displacement curve taken from analysis is illustrated.

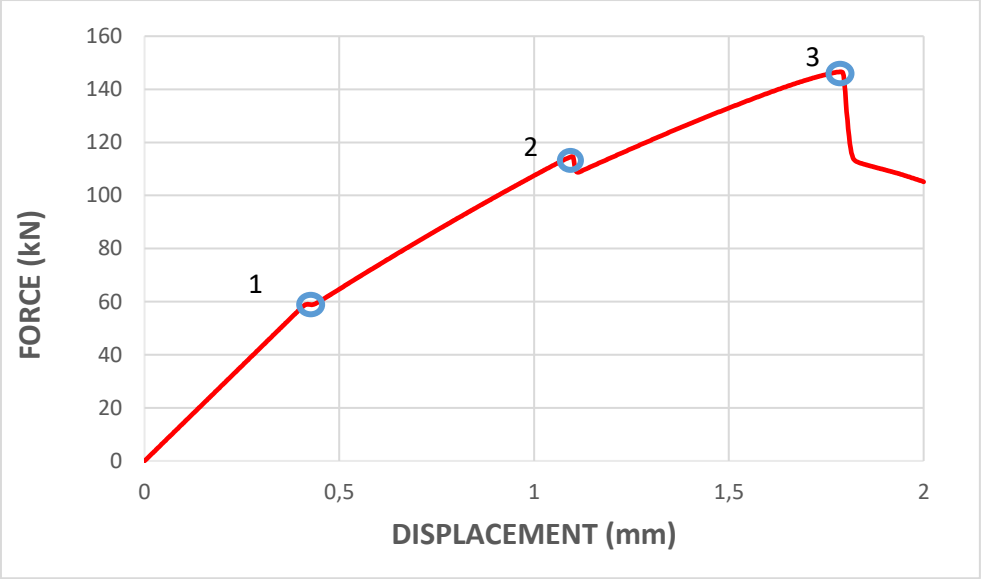

Figure 3.6. Force-Displacement Curve of an Example Analysis

In Figure 3.6, it is seen that the load-displacement curve is a straight line until point 1, and afterward, the slope of the curve decreases slightly, which means the first buckling occurs at point 1 around 60 kN. At points 2, second buckling is observed, and it is around 116 kN. Finally, at point 3, panel strength drops drastically, and the structure loses its load-carrying capacity, which means the stiffened panel is collapsed around 142 kN. Moreover, deformed shapes of the panel at point 1 and point 3 are shown in Figure 3.7.

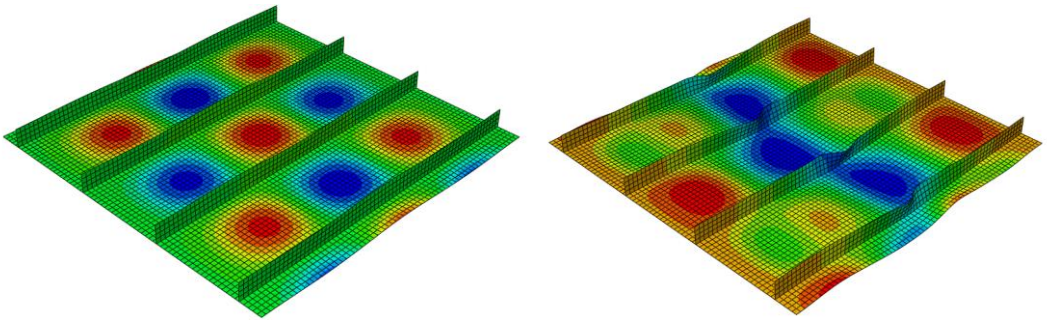

Figure 3.7. Deformed Views of an Example Integrally Stiffened Panel Respectively at Point 1 and Point 3

The first buckling load is extracted by observing the rate of the slope, and the collapse load is taken from the peak value of the reaction force. The mass of the panels is calculated by the mass properties tool of ABAQUS.

3.6 Design Parameter Sensitivity Analysis

As mentioned in Chapter 3.1, six design parameters and three levels of discretization for each specimen are determined to generate the neural network database for integrally stiffened panels. In this chapter, the first buckling and collapse load sensitivity to design parameters of integrally stiffened panels are investigated. For each design parameter, three sample finite element models are generated with changing design levels of the parameter specified in ABAQUS, as mentioned in Chapter 3.3. Note that each time only a single design parameter is changed. For a fair comparison of the sensitivity of each parameter, first buckling and collapse load results are normalized by using the panel weight calculated in each analysis.

In Table 3.3, results for width sensitivity of first buckling and collapse loads of integrally stiffened panels are given, and in Figure 3.8 and Figure 3.9, normalized first buckling and collapse load sensitivity to width is illustrated, respectively.

Table 3.3 First Buckling and Collapse Load Sensitivity to Panel Width

Width [mm]	First Buckling Load [N]	Collapse Load [N]	Mass [gr]	Normalized First Buckling Load [N/gr]	Normalized Collapse Load [N/gr]
350	44348	131665	607	73.06	216.9
400	42975	133886	681	63.10	196.5
450	43748	133451	755	57.94	176.7

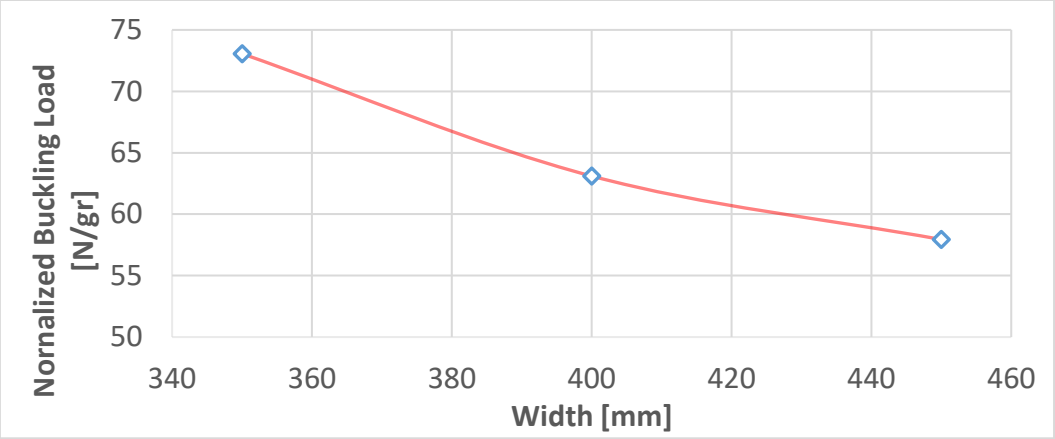

Figure 3.8. First Buckling Load Sensitivity to Panel Width

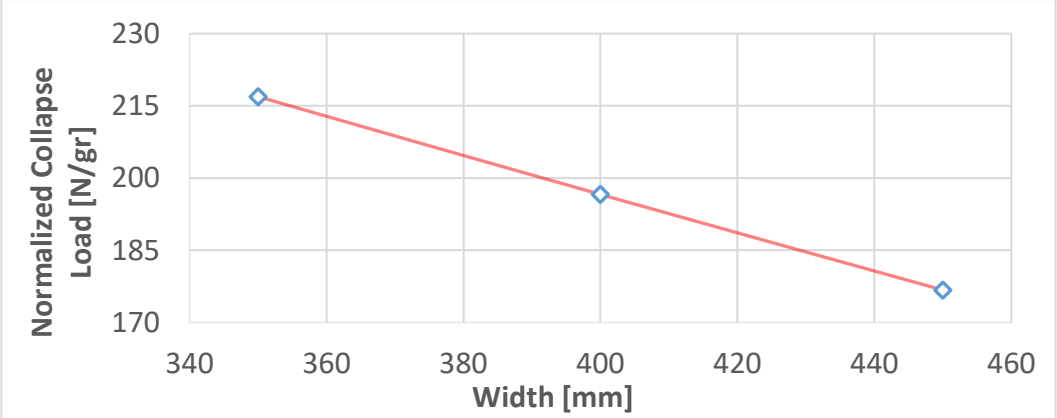

Figure 3.9. Collapse Load Sensitivity to Panel Width

As shown in Figure 3.8 and Figure 3.9, an increase in the panel width decreases the normalized first buckling load of structure from 73 kN/gr to 57 kN/gr and normalized collapse load from 216 kN/gr to 176 kN/gr, which means that buckling characteristics of the structure weakens with increasing panel width.

In Table 3.4, the sensitivity of first buckling and collapse loads to panel skin thickness is given. Figure 3.10 and Figure 3.11 depict the normalized first buckling and collapse loads as a function of panel skin thickness, respectively.

Table 3.4 First Buckling and Collapse Load Sensitivity to Skin Panel Thickness

Skin Panel Thickness [mm]	First Buckling Load [N]	Collapse Load [N]	Mass [gr]	Normalized First Buckling Load [N/gr]	Normalized Collapse Load [N/gr]
1.5	44348	131665	607	73.06	216.9
1.75	62713	163600	693	90.44	235.9
2	83398	188073	779	106.95	241.2

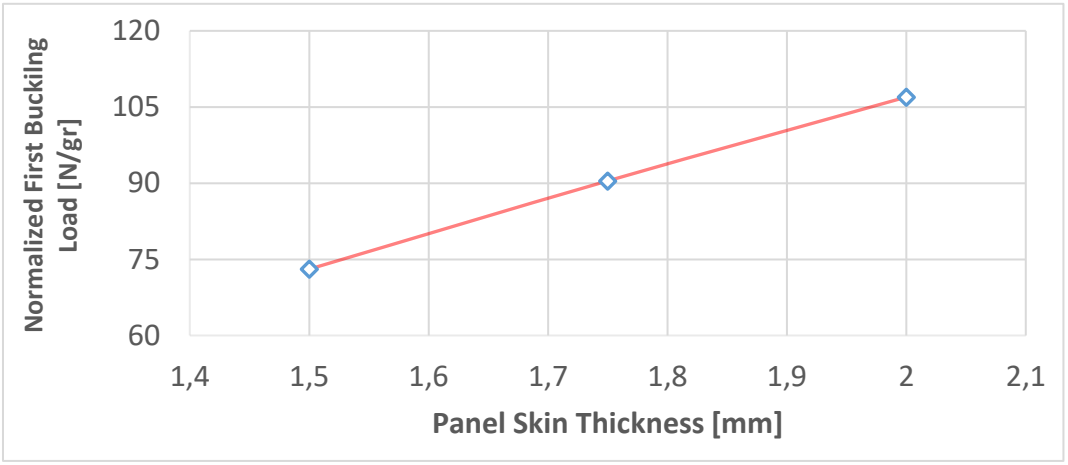

Figure 3.10. First Buckling Load Sensitivity to Skin Panel Thickness

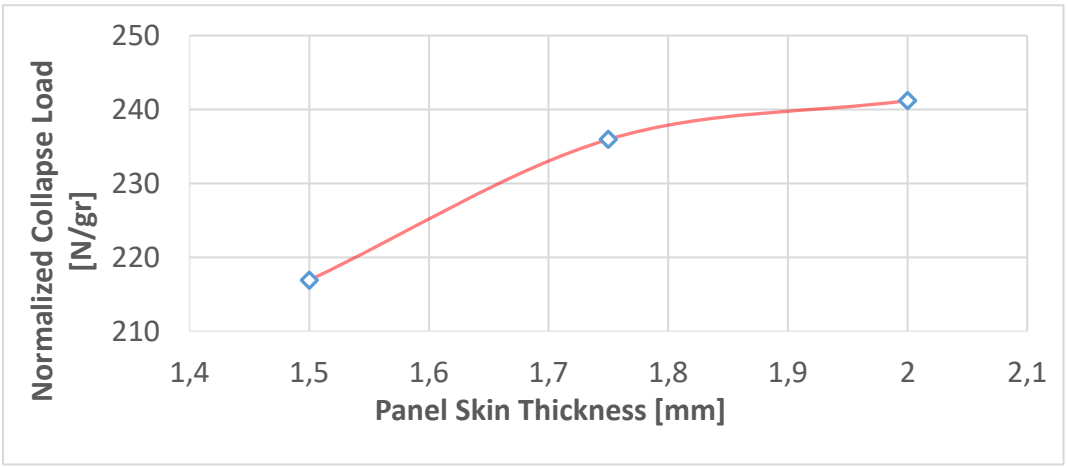

Figure 3.11. Collapse Load Sensitivity to Skin Panel Thickness

As shown in Figure 3.10 and Figure 3.11, an increase in the skin panel thickness increases the normalized first buckling load of structure from 73 kN/gr to 106 kN/gr and the normalized collapse load from 216 kN/gr to 241 kN/gr, which means that buckling characteristics of the structure strengthens with increasing panel width. However, it should be noted that the sensitivity curve for normalized collapse load shows a saturation behavior.

In Table 3.5, results for stringer thickness sensitivity of first buckling and collapse loads of integrally stiffened panels are given. Furthermore, in Figure 3.12 and Figure 3.13, normalized first buckling and collapse load sensitivities to stringer thickness are demonstrated, respectively.

Table 3.5 First Buckling and Collapse Load Sensitivity to Stringer Thickness

Stringer Thickness [mm]	First Buckling Load [N]	Collapse Load [N]	Mass [gr]	Normalized First Buckling Load [N/gr]	Normalized Collapse Load [N/gr]
1.5	44348	131665	607	73.06	216.9
1.75	49909	141170	621	80.26	227.0
2	51660	153568	636	81.14	241.2

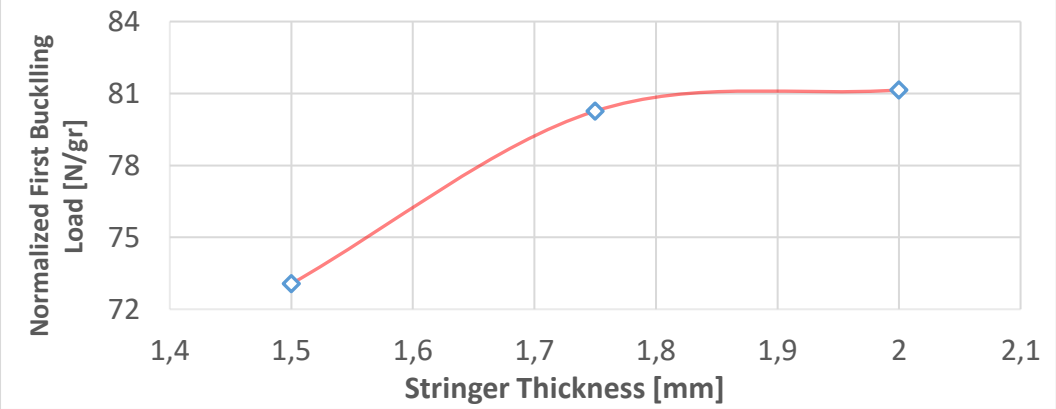

Figure 3.12. First Buckling Load Sensitivity to Stringer Thickness

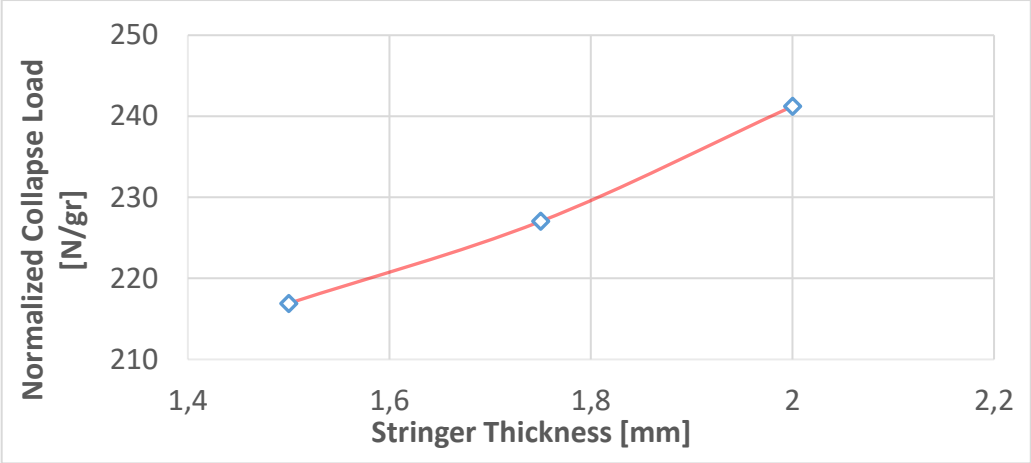

Figure 3.13. Collapse Load Sensitivity to Stringer Thickness

As shown in Figure 3.12 and Figure 3.13, increase in the stringer thickness increases the normalized the first buckling load of structure from 73 kN/gr to 81 kN/gr and normalized collapse load from 216 kN/gr to 241 kN/gr, which means that buckling characteristics of the structure improve with increasing panel width. However, it should be noted that the sensitivity curve for normalized first buckling load exhibits a saturation type response.

In Table 3.6, results for panel length sensitivity of first buckling and collapse loads of integrally stiffened panels are given, and in Figure 3.14 and Figure 3.15, normalized first buckling and collapse load sensitivities to panel length are illustrated, respectively.

Table 3.6 First Buckling and Collapse Load Sensitivity to Panel Length

Panel Length [mm]	First Buckling Load [N]	Collapse Load [N]	Mass [gr]	Normalized First Buckling Load [N/gr]	Normalized Collapse Load [N/gr]
350	44348	131665	607	73.06	216.9
400	42298	130776	693	60.97	188.5
450	39387	126837	780	50.46	162.5

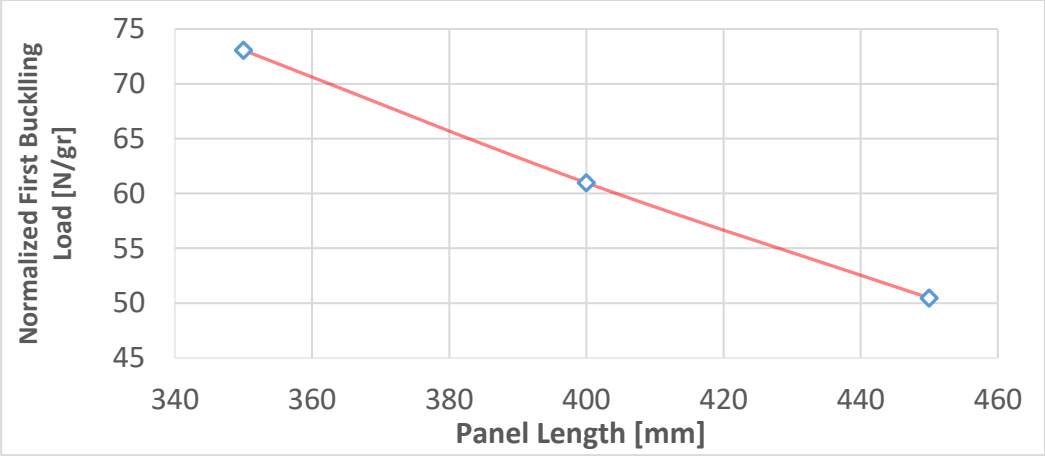

Figure 3.14. First Buckling Load Sensitivity to Panel Length

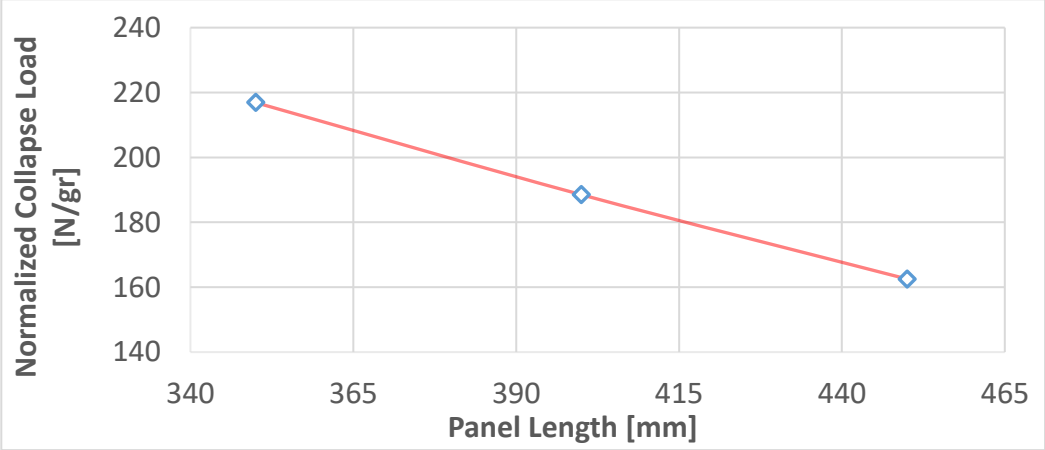

Figure 3.15. Collapse Load Sensitivity to Panel Length

As shown in Figure 3.14 and Figure 3.15, increase in the panel length decreases the normalized first buckling load of structure from 73 kN/gr to 50 kN/gr and thenormalized collapse load from 216 kN/gr to 162 kN/gr, which means that buckling characteristics of the structure weakens with increasing panel width.

In Table 3.7, results for stringer height sensitivity of first buckling and collapse loads of integrally stiffened panels are given, while in Figure 3.16 and Figure 3.17, normalized first buckling and collapse load sensitivities to stringer height are shown, respectively.

Table 3.7 First Buckling and Collapse Load Sensitivity to Stringer Height

Stringer Height [mm]	First Buckling Load [N]	Collapse Load [N]	Mass [gr]	Normalized First Buckling Load [N/gr]	Normalized Collapse Load [N/gr]
15	43139.9	113653	584	73.76	194.3
20	44341.8	132620	607	73.05	218.4
25	45682.1	139509	629	72.60	221.7

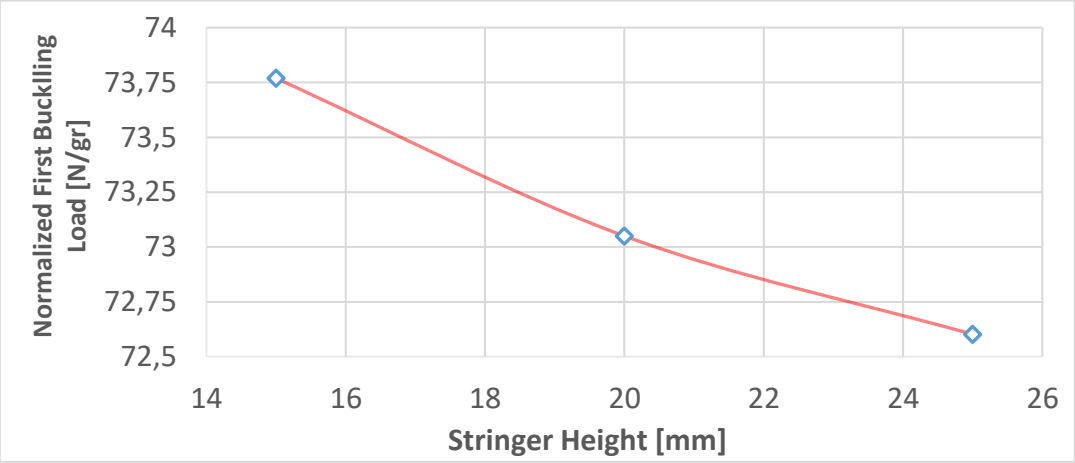

Figure 3.16. First Buckling Load Sensitivity to Stringer Height

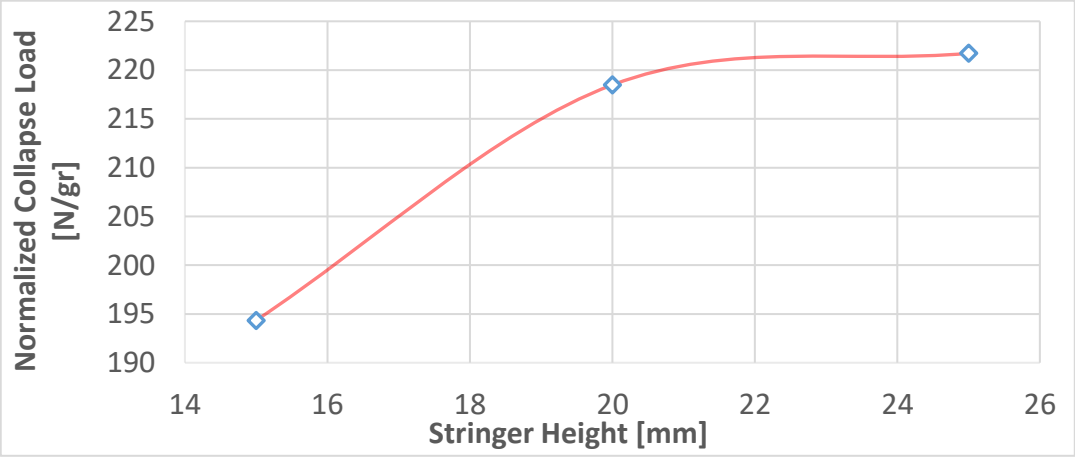

Figure 3.17. Collapse Load Sensitivity to Stringer Height

As shown in Figure 3.16 and Figure 3.17, an increase in the stringer height decreases the normalized first buckling load of structure from 73 kN/gr to 72 kN/gr and increases normalized collapse load from 194 kN/gr to 221 kN/gr. Although there is a slight decrease in the first buckling load of the structure to stringer height, it can be stated that this sensitivity is negligible; therefore, the structure strengthens with increasing stringer height.

In Table 3.8, results for the sensitivity of first buckling and collapse loads to the number of stringers are given. On the other hand, Figure 3.18 and Figure 3.19 depict normalized first buckling and collapse load sensitivities to the number of stringers, respectively.

Table 3.8 First Buckling and Collapse Load Sensitivity to Number of Stringers

Number of Stringers	First Buckling Load [N]	Collapse Load [N]	Mass [gr]	Normalized First Buckling Load [N/gr]	Normalized Collapse Load [N/gr]
3	44348	131665	607	73.06	216.9
4	54067	157011	636	84.92	246.6
5	78714	176131	666	118.14	264.3

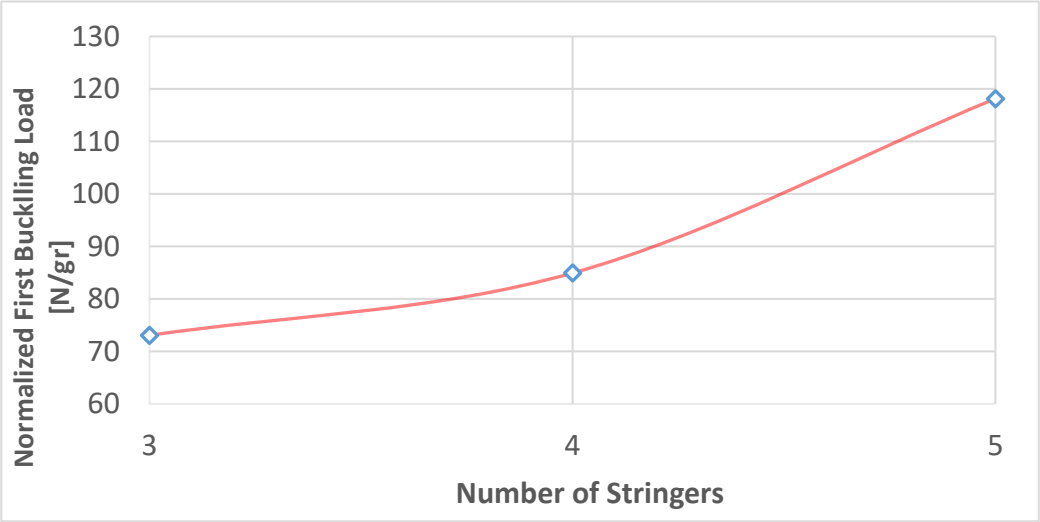

Figure 3.18. First Buckling Load Sensitivity to Number of Stringers

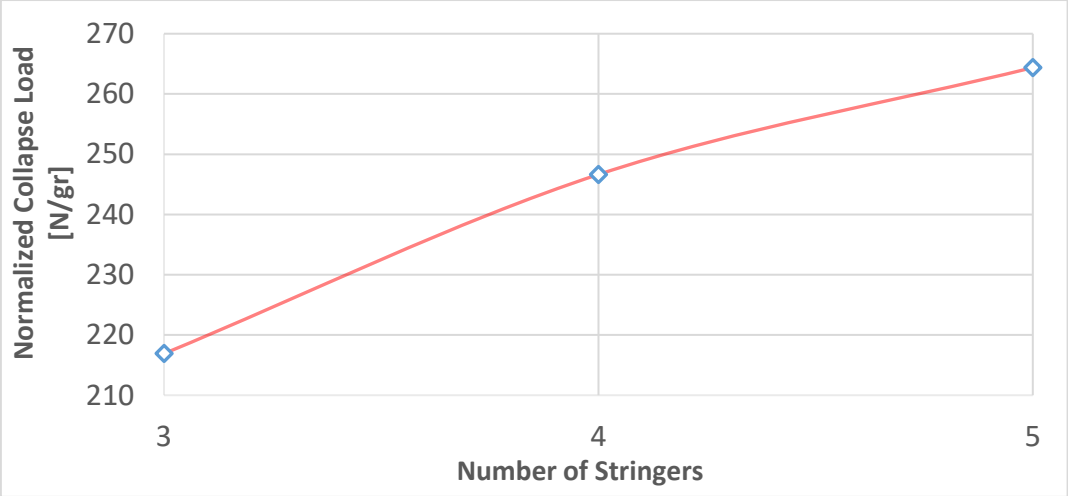

Figure 3.19. Collapse Load Sensitivity to Number of Stringers

As shown in Figure 3.18 and Figure 3.19, an increase in the number of stringers increases the normalized first buckling load of structure from 73 kN/gr to 118 kN/gr and normalized collapse load from 216 kN/gr to 264 kN/gr. It should be noted that with an increase in the number of stringers, the first buckling load increases in a non-convergent manner, whereas the collapse load increases in a slightly convergent fashion.

According to the parameter sensitivity analysis shown above, it can be concluded that the most effective parameter for first buckling and collapse loads of the integrally stiffened panels is the number of stringers. Therefore, the most effective way of increasing the panel strength in terms of buckling characteristics is to increase the number of stringers and the second effective way is to increase panel thickness. Furthermore, the most efficient way of decreasing panel strength can be achieved be increasing panel length or panel width, according to this study.

3.7 Finite Element Analysis Verification

In the verification of the finite element analysis, the study conducted by D. Quinn et al. [35] that involves the test results of a similar integrally stiffened panel structure is considered. A finite element model is created to simulate the test procedure and

analyzed according to Chapter 3.3 and Chapter 3.4. The integrally stiffened test panel dimensions are given in Figure 3.20

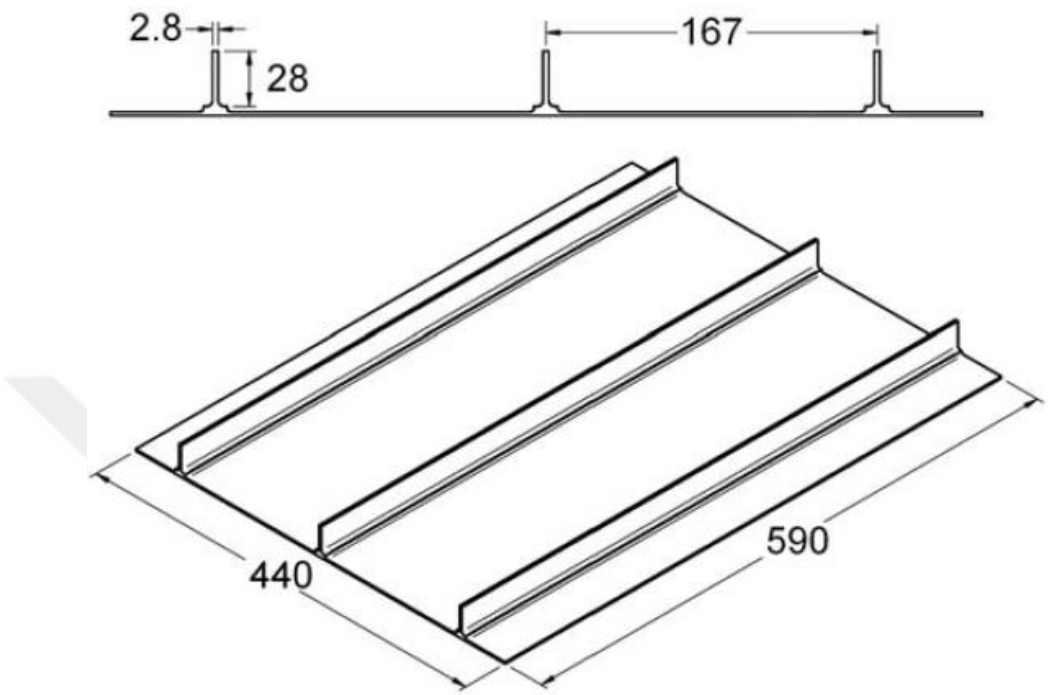

Figure 3.20. Geometric Dimensions of the Integrally Stiffened Test Panel in [35].

The material properties of the test structure are stated in the study as [35]:

- ✓ Elastic Modulus *(E)*: 70000 MPa
- ✓ Poisson's Ratio *(v)*: 0.3
- ✓ Density (ρ): 2.83 g/cm^3
- ✓ Yield Strength (σ_0): 434 MPa
- ✓ Ramberg-Osgood Number (n): 15

The plastic material properties of the test structure are obtained, as explained in Chapter 3.2. The tabulated test results of the study [35] are given with finite element analysis results in Table 3.9.

Table 3.9 Verification Test Results with Finite Element Analysis Results

	First Buckling Load [kN]	Collapse Load [kN]
Test Results	74.5	216.6
Finite Element Analysis	73.4	214.3
Difference (%)	1.48	1.06

According to Table 3.9, the first buckling load of the finite element analysis result is 73.4 kN, which is only 1.48% different from the experimental result [35]. Moreover, the collapse load of the finite element analysis is 214.3 kN, which is 1.06% different from the test result [35]. The finite element analysis followed in this study can therefore be considered as accurate and practical enough to simulate a real-life case.

CHAPTER 4

ARTIFICIAL NEURAL NETWORK

As mentioned in previous chapters, to determine the first buckling and collapse loads of the integrally stiffened structural panels without a need for structural analysis in preliminary design stages, the *Artificial Neural Network (ANN)* tool is used in this study. Moreover, to reduce the time required to create an ANN tool, two different methodologies are used to generate the ANN database. Those methodologies are explained in the following chapters.

Artificial neural networks are instruments for the identification and classification of patterns, and the neural structure of the central nervous system is the basis of ANN. For data estimation, pattern recognition, and optimization, these instruments are primarily used. It is ideal for complex problems that are not adequately solved with conventional mathematical methods because of the high computational capabilities of ANNs [36]. As Haykin [37] described, ANN is a combination of simple processing units that operate in parallel to obtain environmental knowledge by studying and storing the data obtained from the environment within the processing unit links. The learning process is, therefore, an instance of adaptation, manipulated by the environment [38]. Processing devices, which are bio-neuronal analogs, are named “nodes” or “neurons”. Moreover, the strength of interconnection is also called “weight” in an artificial neural network system. As stated in the study of Feldman and Rojas [39], in an artificial neural network, the basic structures of a biological neuron are initiated. The basic structures are known as the information-storing synapses, the cell body that integrates multiple data into a single output, the dendrites that transfer information from synapses to the cell body, and the output-receiving axon. The similarities between an artificial neural network neuron and a biological neuron are shown in Figure 4.1, and it is taken from the study of Gurney [38].

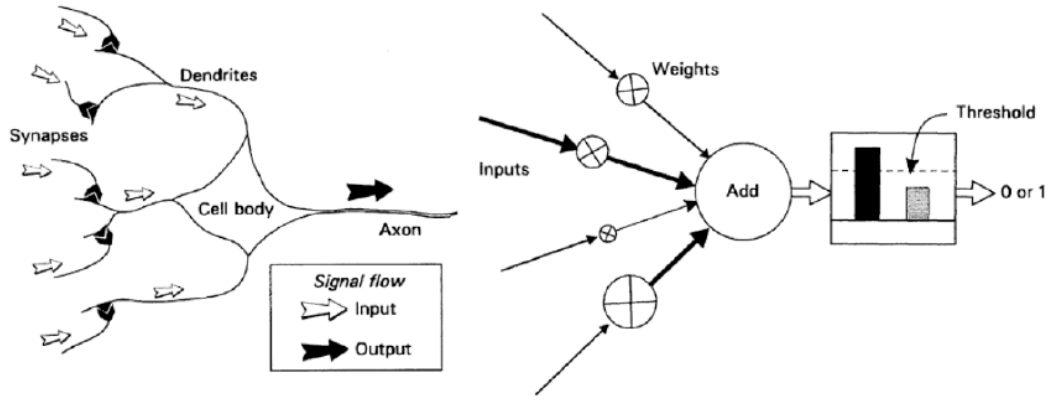

Figure 4.1. A Biological Neuron and an Artificial Neuron [38]

Each input is multiplied by a weight and sent to a feature that in the artificial neuron is a cell body imitation. If the input is above a threshold, the neuron produces a signal. Artificial neurons, working together, build an artificial neural network [40], as illustrated in Figure 4.2.

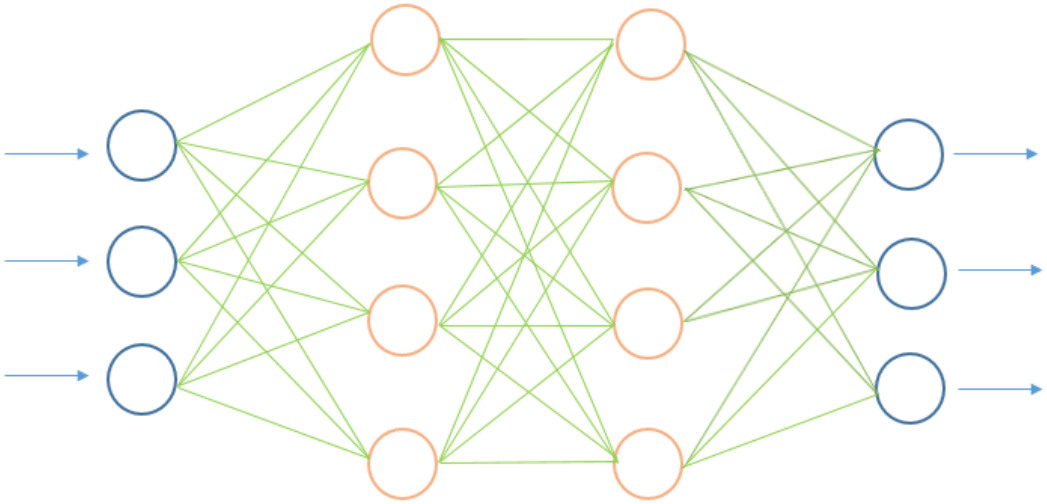

Figure 4.2. Artificial Neural Network

4.1 Theory of Artificial Neural Network

In order to model linear and nonlinear complex systems, ANNs are computational modeling methods. Robustness, fault and noise tolerance, and parallel working capacity are distinct advantages of ANNs, sufficient for nonlinear problems. Besides, ANNs can process imprecise and fuzzy data. Thus, they may provide reliable solutions to ambiguous details. Such capabilities offer essential advantages of excellent data fitting, adaptability, and unlearned data modeling [1]. In this section, brief information about the ANN theory is stated to understand the working mechanism of ANN better.

The artificial neural network produces a mixture of two or more artificial neurons. Numerous interconnections are possible in different ways in the ANN, resulting in countless artificial neural networks' topologies [43]. To build a layer, individual artificial neurons in an artificial neural network are grouped. Then, each layer's neurons are bound to the next layer's neurons. An artificial neural network configuration of 6:48:3 is shown in Figure 4.3.

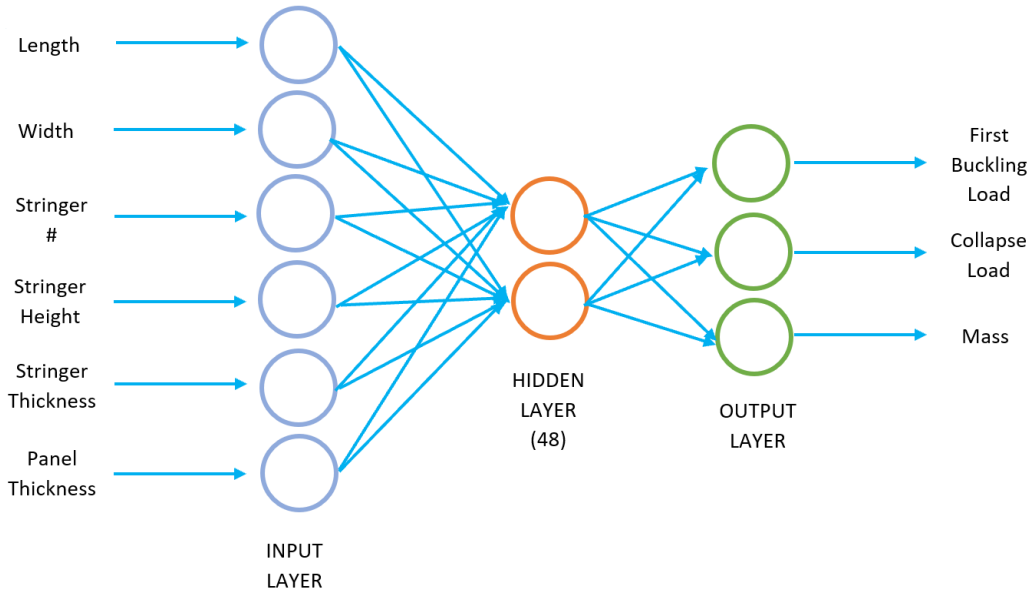

Figure 4.3. ANN with 3:2:1 Configuration

In Figure 4.3, the ANN is composed of three layers. A 3-neuron layer is used to take the system input parameters, a 2-neuron layer or the hidden layer is the output layer that returns two outputs as a result of the computation. The number of input and output parameters is used to determine the number of neurons in the input and output layers. Each neuron is associated with one input or output parameter. The computational capacity of an ANN is then calculated by trial and error to adjust the ANN with the desired capabilities [41].

The MATLAB Neural Network Toolbox includes four types of neural network tools to train a neural network. These are *function fitting* to suit a function, *pattern recognition* to detect and classify an object by tracing its consistency with a given pattern, data clustering to group data based on similarity, and time series analysis to predict an object's future behavior according to information from the past. In this study, the function fitting tool is used to determine the first buckling and collapse loads and mass of integrally stiffened structural panels based on its geometric parameters. MATLAB provides many algorithms to train the artificial neural network, such as Bayesian regulation back-propagation and Resilient back-propagation. However, the Levenberg-Marquardt back-propagation algorithm is recommended, as it is the fastest algorithm among the options provided by the toolbox [42]. Therefore, a feed-forward neural network with Levenberg-Marquardt back-propagation training algorithm is used in this study.

Artificial neurons in an ANN function are building blocks. A neuron's function can be summarized as shown in Figure 4.5 [40], and the corresponding mathematical expression describing the working mechanism of an artificial neuron can be expressed in (4.1). The input i is multiplied by a weight w and a bias b is added to the result. The product of these operations is processed to obtain an output from the neuron in a transfer function f [43].

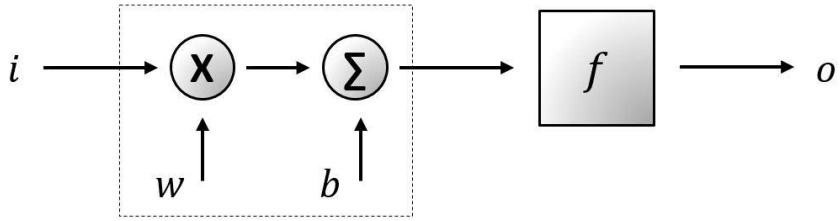

Figure 4.4. Function of an Artificial Neuron [40]

$$f(iw + b) = o \tag{4.1}$$

For each input, the weight and bias are calculated during the ANN training process. The transfer function, therefore, constitutes a major feature of the neuron. Generally, *step function*, a *linear function*, and a *sigmoid function* are the options for the transfer function. The phase function is a feature that can only return one or zero and is used in neurons involved in problems with classification. In neurons that are involved in linear transfer systems, linear functions are used. The sigmoid function is usually used in ANNs-fitting function neurons. It provides outputs between -1 and 1 [42].

4.2 Generation of Artificial Neural Network

ANN requires a database to determine the information required. However, the size of the database is the most critical thing in the training process. It should be large enough to contain sufficient information about a suitable feature but still small enough to provide adequate time for the database to be generated and the ANN to be trained.

To train an ANN, the first parameter to decide in a setting of ANN is the number of hidden layers. The number of hidden layers significantly affects the duration of the training process. In Figure 4.5, the number of neurons is decided by a trial and error aproach as suggested in Chapter 4.1 for the ANN tool used in this study.

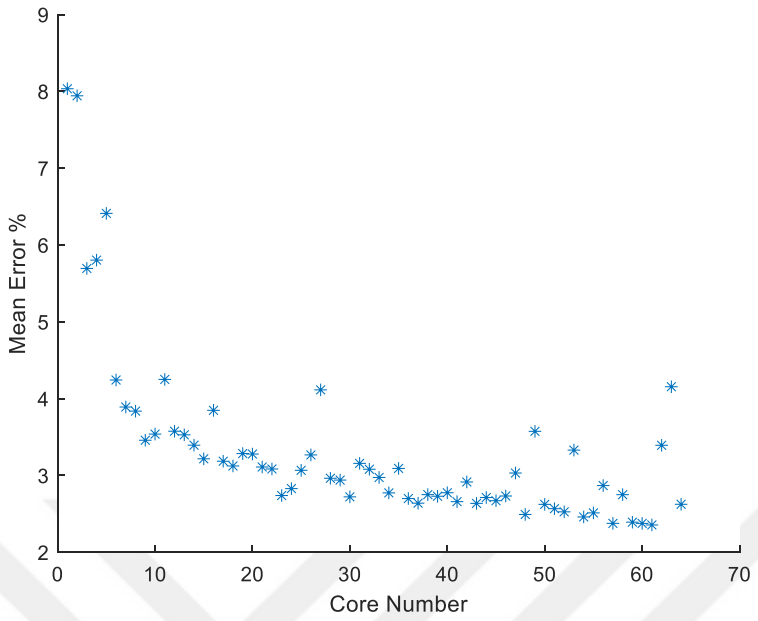

Figure 4.5. Number of Neurons Decision Study Results

As shown in Figure 4.5, ANNs are created by using 2 to 65 neurons, and the results are compared by the mean error percentage. As shown, the most accurate results are reached between 40 and 50 neurons. Then those candidates are compared by the computational time. Altought there is a small difference in comsumed time among the candidates, the fastest and most accurate results are obtained with 48 neurons. Thus, it is deciced to use 48 neurons in the ANN in this study. In Figure 4.6, the generic view of the created ANN with 6:48:3 configuration, which is used throughout this study, can be seen.

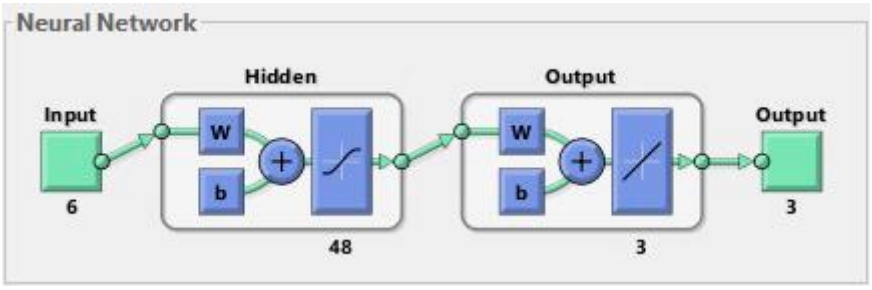

Figure 4.6. Generic View of Neural Network with 48 Neurons

ANN training allows the database to be divided into three parts: the training set, the evaluation set, and the test set. MATLAB divides the data set into 70% for training, 15% for validation, and 15% for default testing [42]. Determining the weights and biases of the neurons is the reason for splitting the database and constructing the training collection. The validation set is used after every iteration of the training phase to verify the precision of the solution. The ANN output is finally tested by the testing set. Thus, 30% of the database is not used for ANN preparation. Not to deprive too many training set data points, percentages of database division are altered as 90% for the training set, 5 percent for the validation set and 5 percent for the test set [40].

Mean Squared Error (MSE) is the measure of training performance. The squared error calculates the squared distance from the fitted line of a data point and provides the MSE with the average of the squared distance. The number of iterations called *Epoch* and the maximum number of iterations without any improvements called *Max Fail* are the termination parameters of the training process. The epoch limit is set to 5000 to prevent early terminations. The Max Fail limit is assigned as 5000.

In this study, two different techniques, namely the *Latin Hypercube Sampling*, a design-of-experiment (DOE) methodology, and the *Multi-fidelity sampling Technique,* are compared with the conventional full-factorial design of experiment approach in terms of accuracy and computational cost.

4.2.1 ANN Generation by Full-factorial Design of Experiment Approach

As given in Table 3.1, there are six design parameters, and each parameter has three levels. The full-factorial approach is a classical design of experiment methodology that uses all possible combinations of design parameters given in Table 3.1. Therefore, according to Table 3.1, there are 729 possible combinations. Thus, the first ANN of this study is created by using all 729 design points. The first buckling

and collapse loads, and the mass information of those design points are calculated using 5 mm mesh size.

4.2.2 ANN Generation by Latin Hypercube Sampling Approach

In order to overcome problems of modern DOE approaches such as non-uniform level of factor requirements or computational cost due to increase in simulation points, the design-of-experiment problem should have a suitable sampling approach. *Latin Hypercube Sampling (LHS)* is a sampling process used to obtain input values to estimate the expectations of output variable functions [44].

The sampling procedure can be formally expressed by following. The range [0,1] divided into N intervals of the equal length $1/N$. A randomly selected point from each interval forms a sequence of *N* points in $H^1\{x_i^1\}, i = 1, \dots, N$. By applying same procedure, an independently constructed second sequence generated as $\{x_i^2\}, i = 1, \dots, N$. These two sequences can be paired to generate a two-dimensional space. This pairs can be can be combined until the n-dimensional squence of N is formed [45]. Mathematical representation is shown in (4.1) [45]. In (4.1), let $\{\pi_k\}$ be independent random permutations of $\{1, \dots, N\}$ each uniformly distributed over all $N!$ possible permutations and U_i^k stands for independently sampled points on [0,1] interval [45].

$$x_i^k = \frac{\pi_k(i)-1+U_i^k}{N}, i = 1, \dots, N \; and \; k = 1, \dots, n \tag{4.1}$$

LHS is a commonly used design-of-experiment technique for design problems that consists of more than two variables. The selected design points are distributed so that they cover all design space but do not intersect each other. Also, the *Latin Hypercube Sampling* ensures that the entire range of each input variable is fully covered, regardless of which single variable or combination of variables may dominate the response of the computer simulation. This means that when certain input variables

dominate some responses, a single sample will provide valuable information, while other input variables dominate other responses. Each variable has the chance to show up as important by sampling over the entire range if it is indeed important. Moreover, in a wide variety of circumstances, LHS is more efficient than simple random sampling [46].

This study aims to have an optimum number of design points in the ANN database, in other words, to reach the most accurate ANN tool with the minimum time consumed. Therefore, the Latin Hypercube Sampling methodology is utilized to achieve that goal. Moreover, sub-spaces with 30%, 60%, and 90% of the full-factorial design space are considered. As in the ANN generated using the full-factorial approach, the first buckling and collapse loads and mass data of the ANNs generated by 30%, 60%, and 90% of the design points are calculated usng 5 mm mesh size. In Chapter 5, the time consumed and the accuracy of the ANNs created by LHS are compared with the ANN created by the full-factorial approach described in Chapter 4.2.1.

4.2.3 ANN Generation by Multi-Fidelity Sampling Approach

In order to have an adequate database for ANN training in a faster way, the next methodology utilized in this study is *Multi-Fidelity Sampling*. The multi-fidelity algorithm aims to reduce the computational time spent for the finite element analyses to generate the ANN database by generating the database from coarse-discretization (low-fidelity) computational models to fine-discretization (high-fidelity) computational models gradually. Figure 4.7 shows an illustrative sketch of the working mechanism of the multi-fidelity sampling methodology [47].

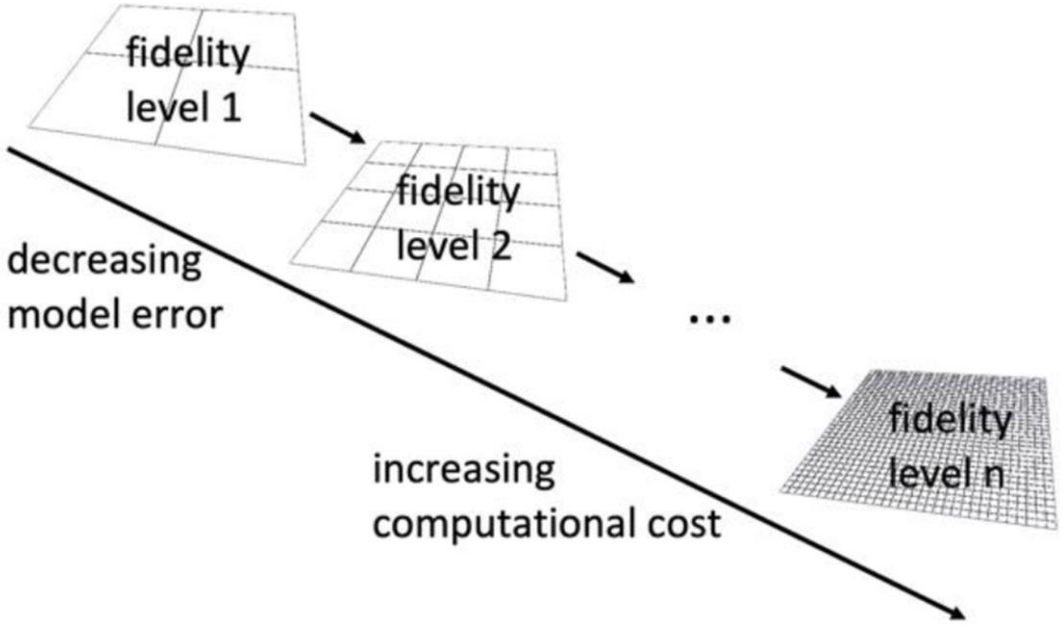

Figure 4.7. Working Mechanism of Multi-Fidelity Sampling Methodology [47]

As shown in Figure 4.7, one needs to define the number of fidelity levels and associated computational models. Then, for each level, finite element analysis data is generated. Afterward, the generated data is implemented to ANN starting from the lowest fidelity level. After the ANN reaches to defined accuracy level, then the next fidelity level is implemented until the defined accuracy level for that fidelity level is reached. Finally, the finest fidelity level data is implemented to the ANN, and the multi-fidelity sampling methodology is completed. As implied, exploiting such a multi-fidelity strategy may substantially reduce overall computational cost. Indeed the main objective of the multi-fidelity sampling methodology is to reduce the computational cost spent for database generation of ANNs [47]. In this thesis, the high-fidelity level stands for finite element analyses performed with fine discretization, whereas the low-fidelity level stands for finite element analyses conducted with coarse discretization.

As stated above, in order to reduce to computational time consumed for the database generation, the multi-fidelity sampling methodology is employed with the Latin hypercube sampling methodology in this study. The reason for employing the Latin hypercube sampling to multi-fidelity sampling is to select data for each fidelity level

in a more distributive manner and increase the accuracy of even low-fidelity training. Moreover, a multi-fidelity sampling with randomly selected data is also performed to see the effects of the LHS on multi-fidelity. The fidelity percentages from coarse mesh data to fine mesh data used in this study are:

- ✓ *30% (coarse)/ 30% (medium)/ 40% (fine) with LHS applied,*
- ✓ *30% (coarse)/ 30% (medium)/ 40% (fine) without LHS applied,*
- ✓ *80% (medium)/ 20% (fine) with LHS applied,*
- ✓ *70% (medium)/ 30% (fine) with LHS applied,*
- ✓ *40% (medium)/ 40% (fine) with LHS applied*
- ✓ *50% (medium)/ 30% (fine) with LHS applied.*

As stated in Chapter 3.3, the fine mesh stands for 5 mm mesh size, whereas the medium mesh is 10 mm and the coarse mesh is 20 mm. These ANNs will be compared agaist each other, against ANNs created by using LHS only, and against ANNs created by the full-factorial approach in Chapter 5.

4.3 Statistical Results of Artificial Neural Networks Generated

Statistical regression analysis results that give information about the data quality for the experiment performed are taken from the *Neural Network* toolbox of MATLAB after each training. Also, the validation performance of the ANN is measured by *Mean Square Error (MSE),* and the validation performance plot of the ANN trained is taken from the MATLAB after each training. In this section, statistical regression analysis results and MSE curves of the database generated by the full-factorial approach are shown to show the quality of the database and validation performance of the ANN generated. It should be noted that the statistical results of the other ANNs generated is not shown since their results are quites similar to the one that is shown.

In Figure 4.8, the validation performance plot of the ANN generated by the full-factorial approach is shown.

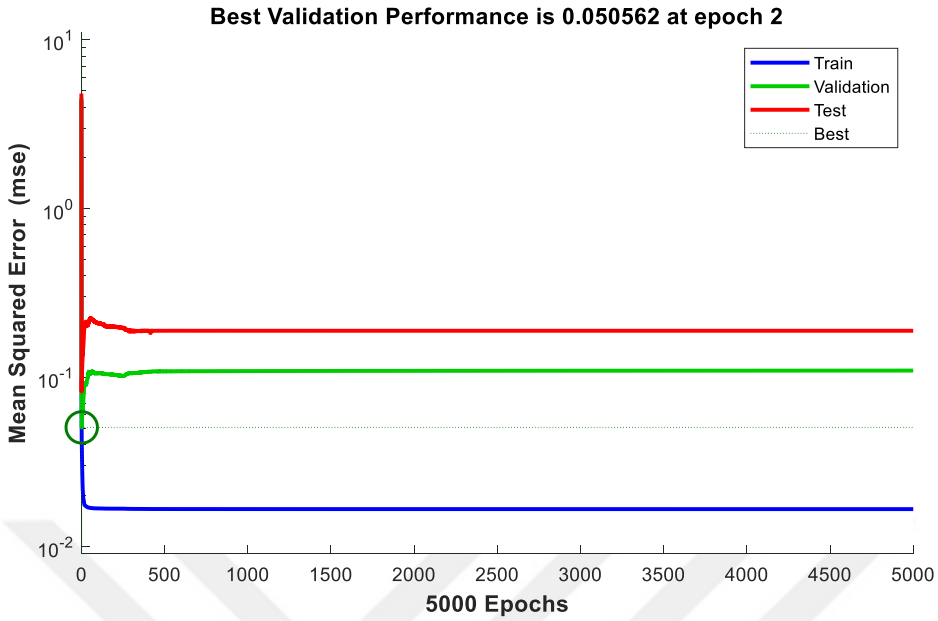

Figure 4.8. Validation Performance Plot of the ANN Generated by Full-Factorial Approach

As shown in Figure 4.8, the mean square error of the ANN is quite small, and the accuracy of the neural network stabilizes itself over iterations, which means that the ANN generated gives convergent results for the determination of the first buckling and collapse loads and mass of target design points.

Figure 4.9 shows the statistical regression analysis of the ANN generated by the full-factorial approach.

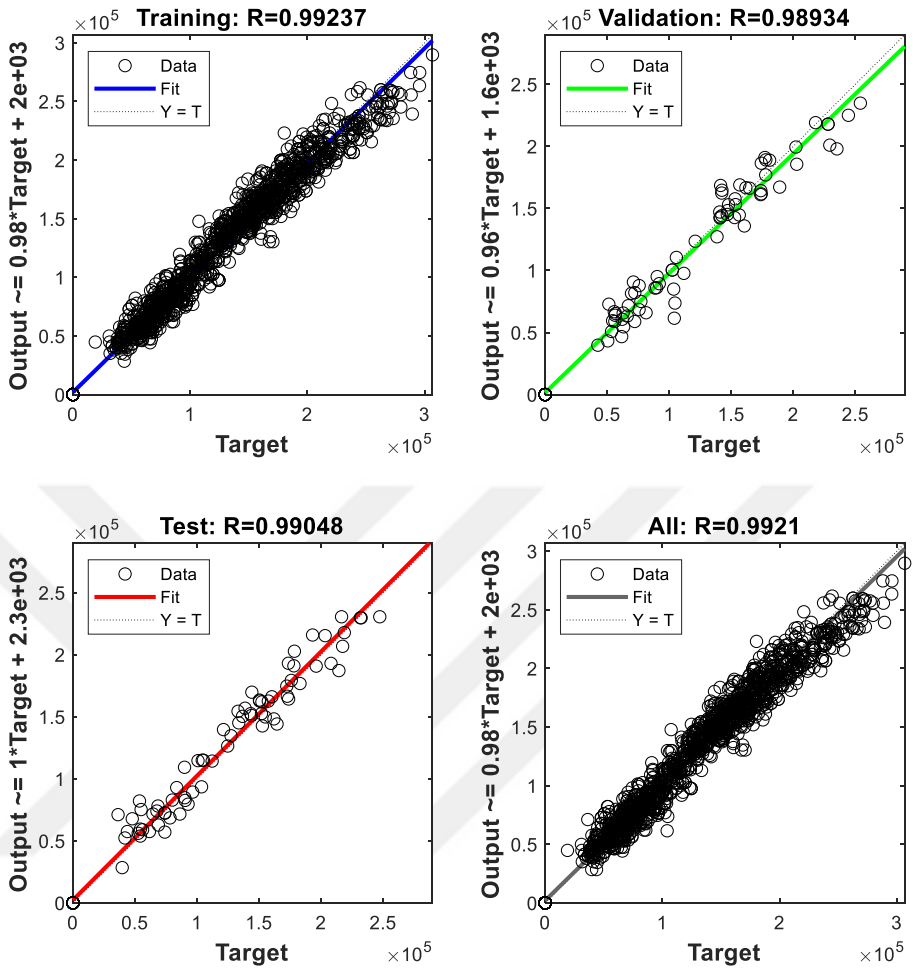

Figure 4.9. Regression Analysis of the ANN Generated by Full-Factorial Approach

In Figure 4.9, vertical axes are the ANN results, and horizontal axes are the FEA results. As shown in Figure 4.9, points create a bold line around the fit curve which means that finite element analysis data used in this study is adequate to determine the output data required. Therefore, it can be concluded from this study that the generated ANN gives promising results.

CHAPTER 5

RESULTS AND COMPARISONS

To classify the result shown in this chapter, the *Fit Performance Model* [48] given in (5.1), *Mean Squared Error*, and *Total Time Spent* for the generation of ANN database are used.

$$FIT = 100\left(1 - \left(\frac{\Sigma(t-dm)^2}{\Sigma\left(t-mean(t)\right)^2}\right)^{1/2}\right) \quad (5.1)$$

In (5.1), t indicates target value, and dm indicates neural network results. Target values are computed with 5 mm FE analyses.

In this chapter, performance parameters of ten ANNs created in this study are investigated individually using randomly selected ten sample data taken from the database. Then, these ANNs are compared by using the performance data mentioned above and the best three participants from three different methodologies are selected. Finally, these three participants are compared using the additional analysis results outside of the database to investigate the ANNs in a real-life application. In Table 5.1, design parameters of randomly selected ten sample panels are given.

Table 5.1 Sample Panel Dimensions

		PANEL DIMENSIONS (mm)					
		LENGTH	WIDTH	STRINGER H.	SKIN T.	STRINGER T.	STRINGER #
EXAMPLE PANEL #	1	350	350	20	2	2	3
	2	350	350	25	2	2	3
	3	350	350	15	2	1.75	3
	4	400	350	20	1.5	1.5	3
	5	400	350	20	2	2	3
	6	400	350	25	2	2	3
	7	450	350	15	1.5	1.5	3
	8	450	350	20	1.5	1.5	3
	9	450	350	25	1.5	1.5	3
	10	450	350	15	1.5	2	3

5.1 Individual Performance Parameters of ANNs Generated

5.1.1 Full-Factorial Approach

ANN results of the full-factorial approach are compared with the fine mesh finite element results for the above-mentioned ten sample panles in Table 5.2.

Table 5.2 Comparison of ANN Results with Reference Finite Element Results for Full-Factorial Approach

		ANALYSIS RESULTS			NEURAL NETWORK RESULTS			ERRORS (%)		
		F_COLLAPSE (N)	F_BUCKLE (N)	MASS (gr)	F_COLLAPSE (N)	F_BUCKLE (N)	MASS (gr)	F_COLLAPSE	F_BUCKLE	MASS
EXAMPLE PANEL #	1	217981.0	99161.0	0.8	216011.6	98469.7	0.8	0.9	0.7	0.4
	2	229107.2	108370.0	0.8	230738.3	107863.8	0.8	0.7	0.5	1.1
	3	163305.2	81181.0	0.8	160251.9	79567.4	0.8	1.9	2.0	0.8
	4	127200.8	48556.0	0.7	126165.2	50527.0	0.7	0.8	4.1	0.3
	5	210629.5	89451.0	0.9	208376.0	91645.8	0.9	1.1	2.5	0.2
	6	215654.8	97623.0	1.0	214609.4	97916.9	1.0	0.5	0.3	0.7
	7	113672.8	41475.0	0.8	115719.3	41432.4	0.8	1.8	0.1	0.9
	8	124977.4	45062.0	0.8	126577.0	43519.0	0.8	1.3	3.4	0.2
	9	132130.8	46793.0	0.8	132090.6	48362.6	0.8	0.0	3.4	0.8
	10	125648.6	50911.0	0.8	126220.3	52041.5	0.8	0.5	2.2	1.6

In Table 5.3, the total time consumed to generate the ANN database, the mean squared error percentage, and the mean fit percentage value are given.

Table 5.3 Performance Parameters of Full-Factorial ANN

	Collapse Load	*First Buckling Load*	*Mass*
Mean Error (%)	2.48	3.07	0.48
Mean Fit (%)	97.52	96.93	99.52
Total Time Spent (sec)		1162935	

According to Table 5.3, the accuracy of the ANN generated by the full-factorial approach is exceptionally good. However, the total time spent to generate the database of the ANN is too much.

5.1.2 Latin Hypercube Sampling

5.1.2.1 ANN Generated by 90% of All Design Points Selected via LHS

In Table 5.4, ANN results generated by using ANN created by 90% of all design points selected via LHS are compared with the reference finite element results.

Table 5.4 Comparison of ANN Results with Reference Finite Element Results for ANN Trained with 90% of All Design Points

		ANALYSIS RESULTS			NEURAL NETWORK RESULTS			ERRORS (%)		
		F_COLLAPSE (N)	F_BUCKLE (N)	MASS (gr)	F_COLLAPSE (N)	F_BUCKLE (N)	MASS (gr)	F_COLLAPSE	F_BUCKLE	MASS
EXAMPLE PANEL #	1	217981.0	99161.0	0.8	218602.7	100926.5	0.8	0.3	1.8	0.0
	2	229107.2	108370.0	0.8	240976.8	121537.3	0.9	5.2	12.2	1.3
	3	163305.2	81181.0	0.8	149974.3	76787.3	0.8	8.2	5.4	0.6
	4	127200.8	48556.0	0.7	124356.8	44670.7	0.7	2.2	8.0	0.5
	5	210629.5	89451.0	0.9	213132.0	79805.4	0.9	1.2	10.8	0.2
	6	215654.8	97623.0	1.0	224335.1	98835.6	1.0	4.0	1.2	0.3
	7	113672.8	41475.0	0.8	115186.1	39454.9	0.8	1.3	4.9	1.1
	8	124977.4	45062.0	0.8	125664.8	46360.2	0.8	0.5	2.9	0.5
	9	132130.8	46793.0	0.8	129550.8	45387.2	0.8	2.0	3.0	0.5
	10	125648.6	50911.0	0.8	126192.3	44547.2	0.8	0.4	12.5	0.0

The total time consumed to generate the ANN database, the mean squared error percentage, and the mean fit percentage values are given in Table 5.5.

Table 5.5 Performance Parameters of ANN Generated by 90% of All Design Points

	Collapse Load	*First Buckling Load*	*Mass*
Mean Error (%)	3.33	6.20	0.65
Mean Fit (%)	96.67	93.79	99.35
Total Time Spent (sec)		1046642	

According to Table 5.5, the accuracy of the ANN generated by using 90% of all design points selected via LHS is satisfactorily good. However, the total time spent to generate the database of the ANN is still too much.

5.1.2.2 ANN Generated by 60% of All Design Points Selected via LHS

Table 5.6 compares ANN results generated by using ANN created by 60% of all design points selected via LHS with the reference finite element results.

Table 5.6 Comparison of ANN Results with Reference Finite Element Results for ANN Trained with 60% of All Design Points

		ANALYSIS RESULTS			NEURAL NETWORK RESULTS			ERRORS (%)		
		F_COLLAPSE (N)	F_BUCKLE (N)	MASS (gr)	F_COLLAPSE (N)	F_BUCKLE (N)	MASS (gr)	F_COLLAPSE	F_BUCKLE	MASS
EXAMPLE PANEL #	1	217981.0	99161.0	0.8	219395.3	101609.9	0.8	0.6	2.5	0.5
	2	229107.2	108370.0	0.8	225407.4	103066.8	0.8	1.6	4.9	0.7
	3	163305.2	81181.0	0.8	157919.7	84002.8	0.8	3.3	3.5	1.3
	4	127200.8	48556.0	0.7	133067.5	53176.1	0.7	4.6	9.5	1.8
	5	210629.5	89451.0	0.9	222533.7	97969.6	0.9	5.7	9.5	1.1
	6	215654.8	97623.0	1.0	226138.0	100957.9	1.0	4.9	3.4	2.0
	7	113672.8	41475.0	0.8	119391.4	38085.8	0.8	5.0	8.2	1.0
	8	124977.4	45062.0	0.8	133338.9	46475.9	0.8	6.7	3.1	0.0
	9	132130.8	46793.0	0.8	138049.8	52206.1	0.8	4.5	11.6	0.1
	10	125648.6	50911.0	0.8	130186.5	51524.3	0.8	3.6	1.2	0.0

Table 5.7 presents the total time consumed to generate the ANN database, the mean squared error percentage, and the mean fit percentage value.

Table 5.7 Performance Parameters of ANN Generated by 60% of All Design Points

	Collapse Load	*First Buckling Load*	*Mass*
Mean Error (%)	3.66	8.24	1.56
Mean Fit (%)	96.34	91.70	98.45
Total Time Spent (sec)		697761	

According to Table 5.7, the ANN's accuracy generated by using 60% of all design points selected via LHS is acceptable. Moreover, the total time spent to generate the database of the ANN is reduced significantly.

5.1.2.3 ANN Generated by 30% of All Design Points Selected via LHS

In Table 5.8, results of ANN trained with 30% of all design points are compared with the reference finite element results.

Table 5.8 Comparison of ANN Results with Reference Finite Element Results for ANN Trained with 30% of All Design Points

		ANALYSIS RESULTS			NEURAL NETWORK RESULTS			ERRORS (%)		
		F_COLLAPSE (N)	F_BUCKLE (N)	MASS (gr)	F_COLLAPSE (N)	F_BUCKLE (N)	MASS (gr)	F_COLLAPSE	F_BUCKLE	MASS
EXAMPLE PANEL #	1	217981.0	99161.0	0.8	200429.5	75127.8	0.8	8.1	24.2	2.6
	2	229107.2	108370.0	0.8	241288.0	84072.8	0.8	5.3	22.4	0.4
	3	163305.2	81181.0	0.8	139575.2	61345.9	0.8	14.5	24.4	0.5
	4	127200.8	48556.0	0.7	132331.5	52765.6	0.7	4.0	8.7	3.1
	5	210629.5	89451.0	0.9	204519.4	73205.1	0.9	2.9	18.2	0.1
	6	215654.8	97623.0	1.0	211537.5	79375.1	1.0	1.9	18.7	0.6
	7	113672.8	41475.0	0.8	126740.6	35880.5	0.8	11.5	13.5	1.0
	8	124977.4	45062.0	0.8	126522.4	44919.9	0.8	1.2	0.3	2.8
	9	132130.8	46793.0	0.8	132330.3	65258.8	0.8	0.2	39.5	1.2
	10	125648.6	50911.0	0.8	139751.1	54046.6	0.8	11.2	6.2	1.1

Table 5.9 shows the total time consumed to generate the ANN database, the mean squared error percentage, and the mean fit percentage values are presented.

Table 5.9 Performance Parameters of ANN Generated by 30% of All Design Points

	Collapse Load	*First Buckling Load*	*Mass*
Mean Error (%)	5.67	15.95	1.05
Mean Fit (%)	94.41	84.09	98.99
Total Time Spent (sec)		348881	

As seen in Table 5.9, the ANN's accuracy generated by using 30% of all design points selected via LHS is reduced, especially for the first buckling load determination. However, the total time spent to generate the database of the ANN is reduced remarkably.

5.1.3 Multi-Fidelity Sampling

5.1.3.1 ANN Trained with 40% Coarse-30% Medium-30% Fine Mesh Analyses Selected with LHS

In Table 5.10, results of ANN trained with 40% coarse mesh-30% medium mesh-30% fine mesh FE analyses are compared with the reference finite element results. Here the LHS is employed for the selection procedure.

Table 5.10 Comparison of ANN Results with Reference Finite Element Results for ANN Trained with 40% Coarse Mesh-30% Medium Mesh-30% Fine Mesh FE Analyses Selected with LHS

		ANALYSIS RESULTS			NEURAL NETWORK RESULTS			ERRORS (%)		
		F_COLLAPSE (N)	F_BUCKLE (N)	MASS (gr)	F_COLLAPSE (N)	F_BUCKLE (N)	MASS (gr)	F_COLLAPSE	F_BUCKLE	MASS
EXAMPLE PANEL #	1	217981	99161	0.8	207223.6	81107.1	0.8	4.9	18.2	1.6
	2	229107.2	108370	0.8	216409.6	101336.5	0.9	5.5	6.5	2.6
	3	163305.2	81181	0.8	160957.7	71476.1	0.8	1.4	12.0	3.8
	4	127200.8	48556	0.7	114252.2	52576.5	0.7	10.2	8.3	0.2
	5	210629.5	89451	0.9	192567.6	74017.4	0.9	8.6	17.3	0.3
	6	215654.8	97623	1	208142.3	93155.2	1.0	3.5	4.6	2.2
	7	113672.8	41475	0.8	110437.4	27659.8	0.7	2.9	33.3	0.4
	8	124977.4	45062	0.8	114980.2	36109.1	0.8	8.0	19.9	0.0
	9	132130.8	46793	0.8	126850.2	43642.4	0.8	4.0	6.7	0.3
	10	125648.6	50911	0.8	133930.5	21621.9	0.8	6.6	57.5	0.3

Table 5.11 give the total time consumed to generate the ANN database, the mean squared error percentage, and the mean fit percentage value.

Table 5.11 Performance Parameters of ANN Trained with 40% Coarse Mesh-30% Medium Mesh-30% Fine Mesh FE Analyses Selected with LHS

	Collapse Load	*First Buckling Load*	*Mass*
Mean Error (%)	6.49	9.78	1.25
Mean Fit (%)	94.67	90.19	98.75
Total Time Spent (sec)		851562	

According to Table 5.11, compared with the full-factorial approach, the accuracy of the ANN trained with 40% coarse/ 30% medium/ 30% fine analyses selected via LHS is reduced, especially for first buckling load determination. However, the total time spent to generate the database of the ANN is respectively less than the total time spent for the full-factorial approach.

5.1.3.2 ANN Trained with 40% Coarse-30% Medium-30% Fine Mesh Analyses Selected with Randomly

In Table 5.12, ANN results of trained with 40% coarse mesh-30% medium mesh-30% fine mesh FE analyses are compared with the reference finite element results. Here the selection procedure is conducted randomly.

Table 5.12 Comparison of ANN Results with Reference Finite Element Results for ANN Trained with 40% Coarse Mesh-30% Medium Mesh-30% Fine Mesh FE Analyses Selected Randomly

		ANALYSIS RESULTS			NEURAL NETWORK RESULTS			ERRORS (%)		
		F_COLLAPSE (N)	F_BUCKLE (N)	MASS (gr)	F_COLLAPSE (N)	F_BUCKLE (N)	MASS (gr)	F_COLLAPSE	F_BUCKLE	MASS
EXAMPLE PANEL #	1	217981	99161	0.8	198958.3	81431.6	0.8	8.7	17.9	1.1
	2	229107.2	108370	0.8	203778.8	95605.1	0.8	11.1	11.8	0.2
	3	163305.2	81181	0.8	143544.6	81467.6	0.8	12.1	0.4	0.6
	4	127200.8	48556	0.7	114923.5	35871.3	0.7	9.7	26.1	1.9
	5	210629.5	89451	0.9	198393.6	75143.9	0.9	5.8	16.0	1.3
	6	215654.8	97623	1	197586.5	89859.3	1.0	8.4	8.0	1.7
	7	113672.8	41475	0.8	107245.7	22857.7	0.8	5.7	44.9	3.6
	8	124977.4	45062	0.8	121321.3	33051.4	0.8	2.9	26.7	5.0
	9	132130.8	46793	0.8	125689.1	40494.0	0.8	4.9	13.5	4.9
	10	125648.6	50911	0.8	133823.6	48870.1	0.8	6.5	4.0	3.5

The total time consumed to generate the ANN database, the mean squared error percentage and the mean fit percentage values are depicted in Table 5.13.

Table 5.13 Performance Parameters of ANN Trained with 40% Coarse Mesh-30% Medium Mesh-30% Fine Mesh FE Analyses Selected Randomly

	Collapse Load	*First Buckling Load*	*Mass*
Mean Error (%)	11.77	10.81	1.45
Mean Fit (%)	91.26	89.32	98.55
Total Time Spent (sec)		862892	

According to Table 5.13, compared with the full-factorial approach, the ANN's accuracy trained with 40% coarse-30% medium-30% fine mesh analyses is reduced, especially for collapse load determination. Also, the total time spent to generate the ANN database is respectively more than the total time spent for the LHS used version.

5.1.3.3 ANN Generated 80% Medium/ 20% Fine Meshed Database Points Selected via LHS

In Table 5.14, ANN results generated by using ANN created by 80% medium/ 20% fine meshed database points selected via LHS are compared with randomly selected database result which are calculated by using fine meshed FE analyses.

Table 5.14 FE Results Comparison with ANN Results for ANN Generated by 80% Medium/ 20% Fine Meshed Database Points Selected via LHS

		ANALYSIS RESULTS			NEURAL NETWORK RESULTS			ERRORS (%)		
		F_COLLAPSE (N)	F_BUCKLE (N)	MASS (gr)	F_COLLAPSE (N)	F_BUCKLE (N)	MASS (gr)	F_COLLAPSE	F_BUCKLE	MASS
EXAMPLE PANEL #	1	217981	99161	0.8	209469.2	98420.8	0.8	3.9	0.7	2.3
	2	229107.2	108370	0.8	221291.5	104914.2	0.9	3.4	3.2	2.0
	3	163305.2	81181	0.8	154665.3	77136.3	0.8	5.3	5.0	1.5
	4	127200.8	48556	0.7	120722.3	51930.1	0.7	5.1	6.9	0.9
	5	210629.5	89451	0.9	209134.9	87630.6	0.9	0.7	2.0	0.0
	6	215654.8	97623	1	218367.5	98257.7	1.0	1.3	0.7	1.0
	7	113672.8	41475	0.8	116337.6	37162.8	0.8	2.3	10.4	1.4
	8	124977.4	45062	0.8	129799.7	44154.2	0.8	3.9	2.0	2.6
	9	132130.8	46793	0.8	135562.5	48059.8	0.8	2.6	2.7	0.1
	10	125648.6	50911	0.8	128038.7	46662.3	0.8	1.9	8.3	0.4

In Table 5.15, total time consumed to generate the ANN database, mean squared error percentage and mean fit percentage value is given.

Table 5.15 Performance Parameters of ANN Generated by 80% Medium/ 20% Fine Meshed Database Points Selected via LHS

	Collapse Load	*First Buckling Load*	*Mass*
Mean Error (%)	3.26	6.63	0.88
Mean Fit (%)	96.78	93.45	99.12
Total Time Spent (sec)		703151	

According to Table 5.15, the accuracy of the ANN generated by using ANN created by 80% medium/ 20% fine meshed database points selected via LHS is increased significantly for all determinations. This increase may be explained by the fact that coarse meshed database points reduce the accuracy of ANN significantly. Also, the total time spent to generate the database of the ANN is significantly less than total time spent for coarse meshed used versions although there is an increase in accuracy.

5.1.3.4 ANN Generated 70% Medium/ 30% Fine Meshed Database Points Selected via LHS

In Table 5.16, ANN results generated by using ANN created by 70% medium/ 30% fine meshed database points selected via LHS are compared with randomly selected database result which are calculated by using fine meshed FE analyses.

Table 5.16 FE Results Comparison with ANN Results for ANN Generated by 70% Medium/ 30% Fine Meshed Database Points Selected via LHS

		ANALYSIS RESULTS			NEURAL NETWORK RESULTS			ERRORS (%)		
		F_COLLAPSE (N)	F_BUCKLE (N)	MASS (gr)	F_COLLAPSE (N)	F_BUCKLE (N)	MASS (gr)	F_COLLAPSE	F_BUCKLE	MASS
EXAMPLE PANEL #	1	217981	99161	0.8	215577.9	94547.7	0.8	1.1	4.7	0.3
	2	229107.2	108370	0.8	219892.3	106449.0	0.8	4.0	1.8	0.9
	3	163305.2	81181	0.8	158372.4	75688.6	0.8	3.0	6.8	0.1
	4	127200.8	48556	0.7	125559.0	48546.3	0.7	1.3	0.0	1.7
	5	210629.5	89451	0.9	211793.5	86454.0	0.9	0.6	3.4	1.3
	6	215654.8	97623	1	214403.7	100477.2	1.0	0.6	2.9	0.4
	7	113672.8	41475	0.8	112777.6	43651.4	0.8	0.8	5.2	0.1
	8	124977.4	45062	0.8	123221.6	41960.1	0.8	1.4	6.9	1.7
	9	132130.8	46793	0.8	131439.4	42626.2	0.8	0.5	8.9	1.1
	10	125648.6	50911	0.8	131016.7	42363.7	0.8	4.3	16.8	0.7

In Table 5.17, total time consumed to generate the ANN database, mean squared error percentage and mean fit percentage value is given.

Table 5.17 Performance Parameters of ANN Generated by 70% Medium/ 30% Fine Meshed Database Points Selected via LHS

	Collapse Load	*First Buckling Load*	*Mass*
Mean Error (%)	3.01	6.05	0.61
Mean Fit (%)	97.08	93.97	99.39
Total Time Spent (sec)		760624	

According to Table 5.17, comparing with *ANN 80/20*, the accuracy of the ANN generated by using ANN created by 70% medium/ 30% fine meshed database points selected via LHS is increased slightly for all determinations. However, total time spent for generation of database is increased.

5.1.3.5 ANN Generated 40% Medium/ 40% Fine Meshed Database Points Selected via LHS

In order to reduce time spent for the database generation and investigate the accuracy for multi-fidelity sampling, 20% of database are excluded. In Table 5.18, ANN results generated by using ANN created by 40% medium/ 40% fine meshed database points selected via LHS are compared with randomly selected database result which are calculated by using fine meshed FE analyses.

Table 5.18 FE Results Comparison with ANN Results for ANN Generated by 40% Medium/ 40% Fine Meshed Database Points Selected via LHS

		ANALYSIS RESULTS			NEURAL NETWORK RESULTS			ERRORS (%)		
		F_COLLAPSE (N)	F_BUCKLE (N)	MASS (gr)	F_COLLAPSE (N)	F_BUCKLE (N)	MASS (gr)	F_COLLAPSE	F_BUCKLE	MASS
EXAMPLE PANEL #	1	217981	99161	0.8	204753.4	92403.0	0.8	6.1	6.8	2.7
	2	229107.2	108370	0.8	225015.2	91276.3	0.8	1.8	15.8	1.1
	3	163305.2	81181	0.8	145479.3	67045.8	0.8	10.9	17.4	2.9
	4	127200.8	48556	0.7	126370.7	61861.3	0.7	0.7	27.4	1.5
	5	210629.5	89451	0.9	218728.8	99961.7	0.9	3.8	11.8	1.3
	6	215654.8	97623	1	219909.8	91460.5	1.0	2.0	6.3	0.3
	7	113672.8	41475	0.8	121530.4	73238.6	0.8	6.9	76.6	2.1
	8	124977.4	45062	0.8	120708.9	58868.8	0.8	3.4	30.6	1.7
	9	132130.8	46793	0.8	129808.3	51563.9	0.8	1.8	10.2	1.5
	10	125648.6	50911	0.8	143351.0	44949.6	0.8	14.1	11.7	0.2

In Table 5.19, total time consumed to generate the ANN database, mean squared error percentage and mean fit percentage value is given.

Table 5.19 Performance Parameters of ANN Generated by 40% Medium/ 40% Fine Meshed Database Points Selected via LHS

	Collapse Load	*First Buckling Load*	*Mass*
Mean Error (%)	3.71	9.02	0.97
Mean Fit (%)	96.33	90.94	99.05
Total Time Spent (sec)		700456	

According to Table 5.19, comparing with *ANN 70/30*, the accuracy of the ANN generated by using ANN created by 40% medium/ 40% fine meshed database points selected via LHS is reduced slightly for all determinations. However, total time spent for generation of database is reduced significantly.

5.1.3.6 ANN Generated 50% Medium/ 30% Fine Meshed Database Points Selected via LHS

In order to reduce time spent for the database generation and investigate the accuracy for multi-fidelity sampling, 20% of database are excluded. In Table 5.20, ANN results generated by using ANN created by 50% medium/ 30% fine meshed database points selected via LHS are compared with randomly selected database result which are calculated by using fine meshed FE analyses.

Table 5.20 FE Results Comparison with ANN Results for ANN Generated by 50% Medium/ 30% Fine Meshed Database Points Selected via LHS

		ANALYSIS RESULTS			NEURAL NETWORK RESULTS			ERRORS (%)		
		F_COLLAPSE (N)	F_BUCKLE (N)	MASS (gr)	F_COLLAPSE (N)	F_BUCKLE (N)	MASS (gr)	F_COLLAPSE	F_BUCKLE	MASS
EXAMPLE PANEL #	1	217981	99161	0.8	203198.2	94594.7	0.8	6.8	4.6	0.1
	2	229107.2	108370	0.8	213741.7	96062.2	0.8	6.7	11.4	0.4
	3	163305.2	81181	0.8	161320.9	82839.3	0.8	1.2	2.0	0.8
	4	127200.8	48556	0.7	126336.1	57777.7	0.7	0.7	19.0	0.3
	5	210629.5	89451	0.9	211421.4	94937.4	0.9	0.4	6.1	2.3
	6	215654.8	97623	1	219457.7	100010.1	1.0	1.8	2.4	3.8
	7	113672.8	41475	0.8	133333.5	39650.1	0.8	17.3	4.4	9.2
	8	124977.4	45062	0.8	133657.3	42357.5	0.8	6.9	6.0	2.4
	9	132130.8	46793	0.8	141466.0	39653.8	0.8	7.1	15.3	3.3
	10	125648.6	50911	0.8	133169.4	45627.9	0.8	6.0	10.4	1.4

In Table 5.21, total time consumed to generate the ANN database, mean squared error percentage, and mean fit percentage value is given.

Table 5.21 Performance Parameters of ANN Generated by 50% Medium/ 30% Fine Meshed Database Points Selected via LHS

	Collapse Load	*First Buckling Load*	*Mass*
Mean Error (%)	4.39	8.51	2.05
Mean Fit (%)	95.62	91.33	97.98
Total Time Spent (sec)		642983	

According to Table 5.21, comparing with *ANN 70/30*, the accuracy of the ANN generated by using ANN created by 50% medium/ 30% fine meshed database points selected via LHS is reduced slightly for all determinations. However, total time spent for generation of database is reduced significantly and it is even less than *ANN 40/40*.

5.2 Comparisons

In this section, ten ANNs generated in this study are compared by total time spent for the database generation, mean squared error percentage, and mean fit percentage value given in Table 5.22.

The first selection between ANNs generated are done by considering following requirements:

- ✓ Total time spent for database generation must be less than 65% of the time spent for database generation of full-factorial ANN.
- ✓ Error percentages must not exceed 7% for any determination.

Table 5.22 General Comparison of ANNs Generated

ANN Type	Total Time Spent (sec)	Mean Error %			Mean Fit %		
		Collapse Load	First Buckling Load	Mass	Collapse Load	First Buckling Load	Mass
Full-Factorial	1162935	2.48	3.07	0.48	97.52	96.93	99.52
90% (LHS)	1046642	3.33	6.20	0.65	96.67	93.79	99.35
60% (LHS)	697761	3,64	8,25	1,16	96,35	91,73	98,85
30% (LHS)	348881	4,31	12,55	1,86	95,75	87,47	98,21
40/30/30 (MF+LHS)	851562	6.49	9.78	1.25	94.67	90.19	98.75
40/30/30 (MF+ Random)	862892	11.77	10.81	1.45	91.26	89.32	98.55
0/80/20 (MF+LHS)	703151	3.26	6.63	0.88	96.78	93.45	99.12
0/70/30 (MF+LHS)	760624	3.01	6.05	0.61	97.08	93.97	99.39
0/40/40 (MF+LHS)	700456	3.71	9.02	0.97	96.33	90.94	99.05
0/50/30 (MF+LHS)	642983	4.39	8.51	2.05	95.62	91.33	97.98

In Table 5.22, the abbreviations *LHS* and *MF* stand for *Latin Hypercube Sampling* and *Multi-fidelity sampling*, respectively. According to Table 5.22, the most accurate results are taken from the ANN generated by using full-factorial approach and it is taken as a reference determinator. However, the most time consumed methodology for the generation of ANN database is the full-factorial approach. To reduce time consumed, two different methodologies are applied. According to Table 5.22, LHS reduces the time required but accuracy of the solutions reduces with reducing number of database points. Therefore, by considering the selection requirements, it can be stated for LHS methodology that, ANN generated by 60% of database points is the most efficient ANN because of the error and fit percentage and time required values. Moreover, multi-fidelity sampling algorithm with LHS applied is also efficient way to reduce the time required to generate ANN database. However, according to Table 5.22, coarse meshed FE analyses reduce the determination accuracy of ANN. In order to clarify the reason, correlation coefficients, which are the covariances of the two different mesh size results divided by multiplication of standard deviation of

each mesh size results given in (5.2), of the finite element analysis results are investigated, and these coefficients are shown below:

$$\rho_{XY} = \frac{cov(X,Y)}{\sigma_X \sigma_Y} \tag{5.2}$$

- ✓ Correlation coefficient between 5 mm and 10 mm for collapse and first buckling loads respectively: 0.98 and 0.97.
- ✓ Correlation coefficient between 5 mm and 20 mm for collapse and first buckling loads respectively: 0.86 and 0.94.
- ✓ Correlation coefficient between 10 mm and 20 mm for collapse and first buckling loads respectively: 0.87 and 0.97.

According to the correlation coefficient analysis, correlation of 20 mm mesh size results is less with the other mesh size results especially for collapse load results. Therefore, in this study only two ANNs are generated by using 20 mm mesh size results and no further combinations with 20 mm mesh size are tested. Also, it should be noted that reducing the sample size for MF trainings reduces the accuracy of the determinations. Therefore, by considering the selection requirements, it can be stated for MF applied ANNs that *ANN 80/20* is the most accurate ANN although it takes more time to generate database comparing with *ANN 50/30*.

As mentioned above, the best three methodologies to generate an ANN database in this study are *Full-Factorial Approach, ANN Generated by 60% of All Design Points Selected via LHS and ANN Generated 80% Medium/ 20% Fine Meshed Database Points Selected via LHS.* These three ANNs then compared by the additional ten design points which are excluded from all design points that generate the database. In Table 5.23, the geometric parameters of additional design points are given in millimeters.

Table 5.23 Geometric Dimensions of Additional Design Points

		PANEL DIMENSIONS (mm)					
		LENGTH	WIDTH	STRINGER H.	SKIN T.	STRINGER T.	STRINGER #
EXAMPLE PANEL #	1	500	500	30.0	1.2	1.20	3
	2	375	375	22.5	1.5	1.50	3
	3	425	400	22.5	1.5	1.75	3
	4	475	400	30.0	3.0	1.75	3
	5	500	500	27.5	2.0	2.50	3
	6	300	300	17.0	1.8	1.50	4
	7	350	350	30.0	2.5	2.00	4
	8	425	400	17.5	1.8	2.25	4
	9	400	350	20.0	1.5	3.00	5
	10	350	300	15.0	2.5	2.50	5

In Table 5.24, Table 5.25 and Table 5.26, ANN results generated by using ANN created by *Full-Factorial Approach, ANN Generated by 60% of All Design Points Selected via LHS and ANN Generated 80% Medium/ 20% Fine Meshed Database Points Selected via LHS*, are compared respectively by taking ANN generated by full-factorial approach as reference determinator with results additional design points which are calculated by using fine meshed FE analyses.

Table 5.24 FE Results of Additional Design Points Comparison with ANN Results for ANN Generated Full-factorial Approach.

		ANALYSIS RESULTS			NEURAL NETWORK RESULTS			ERRORS (%)		
		F_COLLAPSE (N)	F_BUCKLE (N)	MASS (gr)	F_COLLAPSE (N)	F_BUCKLE (N)	MASS (gr)	F_COLLAPSE	F_BUCKLE	MASS
EXAMPLE PANEL #	1	95418.2	28116.0	1.0	84724.2	22891.2	0.9	11.2	18.6	11.9
	2	132881.9	49178.0	0.7	139809.0	53544.1	0.7	5.2	8.9	2.0
	3	145044.7	45632.0	0.9	146434.3	51122.5	0.8	1.0	12.0	2.9
	4	293367.7	223000.0	1.8	262571.7	167072.0	1.4	10.5	25.1	20.8
	5	259220.7	126930.0	1.7	254861.3	120201.1	1.4	1.7	5.3	19.2
	6	173504.2	92691.0	0.5	133729.2	67490.8	0.6	22.9	27.2	10.1
	7	343628.3	205560.0	1.1	294327.2	182996.4	1.1	14.3	11.0	0.0
	8	199534.2	73434.0	1.0	224678.6	96554.7	1.0	12.6	31.5	0.8
	9	262696.3	150570.0	0.9	251587.4	118198.7	1.0	4.2	21.5	3.2
	10	266926.3	228150.0	0.9	223684.9	169761.5	1.1	16.2	25.6	20.1

Table 5.25 FE Results of Additional Design Points Comparison with ANN Results for ANN Generated by 60% of Design Points Selected by LHS

		ANALYSIS RESULTS			NEURAL NETWORK RESULTS			ERRORS (%)		
		F_COLLAPSE (N)	F_BUCKLE (N)	MASS (gr)	F_COLLAPSE (N)	F_BUCKLE (N)	MASS (gr)	F_COLLAPSE	F_BUCKLE	MASS
EXAMPLE PANEL #	1	95418.2	28116.0	1.0	145105.0	30656.9	1.0	52.1	9.0	0.5
	2	132881.9	49178.0	0.7	149136.5	50159.0	0.7	12.2	2.0	2.7
	3	145044.7	45632.0	0.9	148721.6	57887.5	0.9	2.5	26.9	1.0
	4	293367.7	223000.0	1.8	303628.2	139324.2	1.4	3.5	37.5	25.7
	5	259220.7	126930.0	1.7	248023.0	180660.8	1.4	4.3	42.3	18.3
	6	173504.2	92691.0	0.5	118277.5	52874.8	0.6	31.8	43.0	4.7
	7	343628.3	205560.0	1.1	294515.9	143487.0	1.1	14.3	30.2	2.4
	8	199534.2	73434.0	1.0	213956.5	90579.4	1.0	7.2	23.3	1.8
	9	262696.3	150570.0	0.9	273850.9	136268.0	0.9	4.2	9.5	0.2
	10	266926.3	228150.0	0.9	240367.6	145764.9	0.9	9.9	36.1	3.0

Table 5.26 FE Results of Additional Design Points Comparison with ANN Results for ANN Generated by 80% Medium / 20% Fine Meshed Design Points Selected by LHS

		ANALYSIS RESULTS			NEURAL NETWORK RESULTS			ERRORS (%)		
		F_COLLAPSE (N)	F_BUCKLE (N)	MASS (gr)	F_COLLAPSE (N)	F_BUCKLE (N)	MASS (gr)	F_COLLAPSE	F_BUCKLE	MASS
EXAMPLE PANEL #	1	95418.2	28116.0	1.0	158929.4	42799.7	1.0	66.6	52.2	2.8
	2	132881.9	49178.0	0.7	131404.9	57039.0	0.7	1.1	16.0	3.4
	3	145044.7	45632.0	0.9	153505.4	55479.7	0.9	5.8	21.6	0.9
	4	293367.7	223000.0	1.8	249470.2	156116.9	1.5	15.0	30.0	20.0
	5	259220.7	126930.0	1.7	247642.9	157883.9	1.3	4.5	24.4	21.5
	6	173504.2	92691.0	0.5	121377.1	48196.5	0.6	30.0	48.0	14.8
	7	343628.3	205560.0	1.1	260377.4	200185.2	1.2	24.2	2.6	7.9
	8	199534.2	73434.0	1.0	216979.4	101721.5	1.0	8.7	38.5	2.9
	9	262696.3	150570.0	0.9	262427.2	158768.5	0.9	0.1	5.4	1.1
	10	266926.3	228150.0	0.9	237908.7	278074.9	1.1	10.9	21.9	23.9

In Table 5.27, Table 5.28, and Table 5.29, mean squared error percentage and mean fit percentage values for addtional analysis results of *Full-Factorial Approach, ANN Generated by 60% of All Design Points Selected via LHS and ANN Generated 80% Medium/ 20% Fine Meshed Database Points Selected via LHS*, are given respectively.

Table 5.27 Performance Parameters of ANN Generated Full-Factorial Approach

	Collapse Load	*First Buckling Load*	*Mass*
Mean Error (%)	9.99	18.66	9.09
Mean Fit (%)	90.01	81.34	90.91

Table 5.28 Performance Parameters of ANN Generated by 60% of Selected Design Points via LHS

	Collapse Load	*First Buckling Load*	*Mass*
Mean Error (%)	14.22	25.99	6.04
Mean Fit (%)	85.78	74.01	93.96

Table 5.29 Performance Parameters of ANN Generated by 80% Medium/ 20% Fine Meshed Database Points Selected via LHS

	Collapse Load	*First Buckling Load*	*Mass*
Mean Error (%)	16.69	26.06	9.94
Mean Fit (%)	83.31	73.94	90.06

As shown in Table 5.27, Table 5.28 and Table 5.29, the most accurate way to create an artificial neural network is the ANN generated by full-factorial approach.

However, time spent to generate the ANN database is too much. Altough the solution accuracy reduces, the most efficient way to generate the ANN database is the ANN created by appliying design of experiment methodology called *Latin Hypercube Sampling.* By selecting the database points by LHS can reduce the database generation time significantly with slight reduce in determination accurracy. Moreover, application of multi-fidelity sampling algorithm gives similarly accurate results compared to the LHS applied version. However, number of database points required is more than the LHS applied version. To conclude, according to the results of this study, most efficient ANN tool is chosen as *ANN generated by 60% of selected design points via LHS.*

CHAPTER 6

CONCLUSION AND FUTURE WORKS

6.1 Conclusion

This study aims to generate an artificial neural network-based tool to determine the mass, the first buckling, and collapse loads of integrally stiffened structural panels, which are commonly used in today's aerospace industry.

To achive the aim, a database is needed to create ANN. However, the time required to generate the database with the desired accuracy would be too cotly since there are 729 design points to be analyzed with the FE method. Therefore, other than the conventional full-factorial design of experiment approach, special ways to generate this database are investigated in this study. The Latin Hypercube sampling is one of these special design of experiment methodologies. The LHS aims to select database points to cover the whole design space but do not intersect with each other. Therefore, three different configurations, which consist of 90%, 60%, and 30% of design points selected via LHS, are implemented to generate the ANN database. Then ANNs generated are tested by using fine mesh FE anaylsis results. A multi-fidelity sampling algorithm is also considered another way to generate the ANN database in this study. The multi-fidelity algorithm suggests generating the database incrementally by changing the data fidelity. Therefore, sizx different configurations, which are 40% coarse mesh-30% medium mesh-30% fine mesh database with LHS, 40% coarse mesh-30% medium mesh-30% fine mesh database without LHS, 80% medium mesh-20% fine mesh database with LHS, 70% medium mesh-30% fine mesh database with LHS, 40% medium mesh-40% fine mesh database with LHS, and 50% medium mesh-30% fine mesh database with LHS are used to train the ANN. Then the ANNs generated are tested by using fine mesh FE analysis results.

According to the results, it can be stated that the selected design of experiment methodologies and the multi-fidelity algorithm can reduce the total time spent to generate an ANN database significantly. However, the accuracy of the determinations drops with a reducing number of database points. Therefore, one should implement the LHS and multi-fidelity sampling algorithm by considering the desired accuracy. Since this tool is a preliminary design tool, determination accuracy should be about 95-90%. Therefore, according to the comparisons conducted in this study, the most efficient way to create a database of this tool is to apply LHS for the database point selection procedure.

Finally, according to the results mentioned previously, the tool's mass determination is the most accurate since the most stable data is the mass in the ANN database. Moreover, the tool's first buckling load determination is the worst because of the unstable physical nature of the buckling phenomenon. The ANN tool generated in this study gives satisfactorily accurate results for randomly selected design points inside and outside of the database limits if the training database is properly generated. However, one should note that the accuracy of the determinations reduces remarkably as the design target gets far from the database limits.

6.2 Future Works

The structural analysis performed in this study contains only a single type of loading that is compression. However, this tool can be created for other types of loadings such as shear or combined shear and compression. Then, applying the procedures given in this study can widen the scope of the ANN tool. Moreover, in this study, three different configurations are used for the application of Latin hypercube sampling. By testing different sampling configurations, more efficient database sizes can be achieved. Likewise, in this study, six different configurations are used for the application of a multi-fidelity sampling algorithm. By testing different fidelity percentages, more efficient database sizes can be achieved. Moreover, this study can be performed by using 15 mm mesh size analysis results as coarse results so that an

ANN which has three different fidelity level can be more accurate. A self learning algorithm for multi-fidelity sampling algorithm can be generated and applied. Also, different design of experiment methodologies can be applied to search for the most accurate design of experiment methodology for this type of experiment.

Moreover, in this study, integrally stiffened panels used are made of aluminum only. However, this tool can also be created for different materials, such as composite integrally stiffened structural panels. Finally, the database size can be enlarged so that the solution accuracy of the ANNs generated in this study increases.

REFERENCES

[1] I. A. Basheer and M. Hajmeer. Artificial Neural Networks: Fundamentals, Computing, Design, and Application. Journal of Microbiological Methods, 43(1):3–31, 2000.

[2] S. M. El-Soudani. Methods of Making Integrally Stiffened Axial Load Carrying Skin Panels for Primary Aircraft Structure and Fuel Tank Structures. United States Patent. Patent No: US007093470B2, August 2006.

[3] J. Munroe, K. Wilkins, and M. Gruber. Integrally Airframe Structures (IAS) – Validated Feasibility Study of Integrally Stiffened Metallic Fuselage Panels for Reducing Manufacturing Cost. NASA/CR-2000-209337. May 2000.

[4] M.M. Alinia, H.R. Habashi, and A. Khorram. Nonlinearity in the Postbuckling Behaviour of Thin Steel Shear Panels. Thin-Walled Structures, 47(4):412–420, 2009.

[5] K.K. Choong and E. Ramm. Simulation of Buckling Process of Shells by Using the Finite Element Method. Thin-Walled Structures, 31(1):39–72, 1998.

[6] P. S. Ferreira and F. B.E. Virtuoso. Semi-Analytical Models for the Post-Buckling Analysis and Ultimate Strength Prediction of Isotropic and Orthotropic Plates Under Uniaxial Compression with the Unloaded Edges Free from Stresses. Thin- Walled Structures, 82:82–94, 2014.

[7] M. Muameleci. Linear and Nonlinear Buckling Analyses of Plates Using the Finite Element Method. Master's Thesis, Linköping University, Linköping, Sweden, June 2014.

[8] M. Amani, B.L.O. Edlund, and M.M. Alinia. Buckling and Post Buckling Behavior of Unstiffened Slender Curved Plates Under Uniform Shear. Thin-Walled Structures, 49(8):1017–1031, 2011.

[9] E. Aydin, A. Kayran. Comparative Study of Post-Buckling Load Redistribution in Stiffened Aircraft Panel with and without Material Nonlinearity.

International Mechanical Engineering Congress & Exposition. November 9-15. 2018. Pittsburgh, Pennsylvania. USA.

[10] C. Lynch, A. Murphy, M. Price, and A. Gibson. The Computational Post Buckling Analysis of Fuselage Stiffened Panels Loaded in Compression. Thin- Walled Structures, 42(10):1445–1464, 2004.

[11] A. Murphy, M. Price, C. Lynch, and A. Gibson. The computational post buckling analysis of fuselage stiffened panels loaded in shear. Thin-Walled Structures, 43(9):1455–1474, 2005.

[12] J. Campbell, L. Hetey, and R. Vignjevic. Non-linear Idealisation Error Analysis of a Metallic Stiffened Panel Loaded in Compression. Thin-Walled Structures, 54:44–53, 2012.

[13] Y. Wang. Virtual Testing of Post-Buckling Behaviour of Metallic Stiffened Panel. Master's Thesis, Cranfield University, Cranfield, England, 2011.

[14] Peng Hao, Dachuan Liu, Kunpeng Zhang, Ye Yuan, Bo Wang, Gang Li, Xi Zhang, Intelligent layout design of curvilinearly stiffened panels via deep learning-based method, Materials & Design, Volume 197, 2021, 109180, 2020.

[15] C. Bisagni and L. Lanzi. Post-Buckling Optimisation of Composite Stiffened Panels Using Neural Networks. Composite Structures, 58(2):237–247, 2002

[16] M. R. Sheidaii and R. Bahraminejad. Evaluation of Compression Member Buckling and Post-Buckling Behavior Using Artificial Neural Network. Journal of Constructional Steel Research, 70:71–77, 2012.

[17] A. Cankur, E. Gürses, "Development of an Artificial Neural Network Based Analysis Method for Skin-Stringer Structures", 7th EASN International Conference on Innovation in European Aeronautics Research, September 26-29, 2017, Warsaw, Poland.

[18] A. Yıldırım, A. A. Akay, H. Gülaşık, E. Gürses, D. Çöker, A. Kayran, "Development of Bolted Flange design Tool Based on Finite Element Analysis and Artificial Neural Networks", IMECE2015 - ASME 2015 International Mechanical Engineering Congress & Exposition, November 13-19, 2015, Houston, Texas, USA.

[19] A. Yıldırım, A. A. Akay, H. Gülaşık, D. Çoker, E. Gürses, A. Kayran, "Development of Bolted Flange Design Tool Based on Artificial Neural Network", Journal of Pressure Vessel Technology, vol. 141, 052013, 2019.

[20] H. M. Gomes, A. M. Awruch, and P. A. M. Lopes. Reliability Based Optimization of Laminated Composite Structures Using Genetic Algorithms and Artificial Neural Networks. Structural Safety, 33(3):186–195, 2011.

[21] A. Okul, E. Gürses, "Development of Structural Neural Network Design Tool for Buckling Behaviour of Skin-Stringer Structures Under Combined Compression and Shear Loading", IMECE 2018 - ASME 2018 International Mechanical Engineering Congress & Exposition, November 9-15, 2018, Pittsburgh, Pennsylvania, USA.

[22] Z. Sadovský and C. G. Soares. Artificial Neural Network Model of the Strength of Thin Rectangular Plates with Weld Induced Initial Imperfections. Reliability Engineering & System Safety, 96(6):713–717, 2011. ESREL 2009 Special Issue.

[23] L. Lanzi and V. Giavotto. Post- -Buckling Optimization of Composite Stiffened Panels: Computations and Experiments. Composite Structures, 73(2):208–220, 2006. International Conference on Buckling and Post-Buckling Behavior of Composite Laminated Shell Structures.

[24] U. K. Mallela and A. Upadhyay. Buckling Load Prediction of Laminated Composite Stiffened Panels Subjected to In-Plane Shear Using Artificial Neural Networks. Thin-Walled Structures, 102:158–164, 2016.

[25] A. M. J. Olsson and G. E. Sandberg. Latin Hypercube Sampling for Stochastic Finite Element Analysis. Journal of Engineering Mechanics. Vol. 128 Issue 1. January 2002

[26] K. Ding, Z. Zhou, and C. Liu. Latin Hypercube Sampling Used in the Calculation of the Fracture Probability. Reliability Engineering and System Safety. Vol. 59 Issue 2 Pg. 239-242. February 1998.

[27] R. Ferrari, D. Froio, E. Rizzi, C. Gentile and E. N. Chatzi. Model Updating of a Historic Concrete Bridge by Sensitivity and Global Optimization Based Latin Hypercube Sampling. Engineering Structures. Vol. 44 Pg. 336-344. January 2019.

[28] E. Huang, J. Xu, S. Zhang and C. H. Chen. Multi-Fidelity Model Integration for Engineering Design. Procedia Computer Science. Vol. 179 Pg. 139-160. 2015.

[29] D. Böhnke, B. Nagel and V. Gollnick. An Approach to Multi-Fidelity in Conceptual Aircraft Design in Distributed Design Environments. IEEE. April 2011.

[30] K. Yoo, O. Bacarezza and M. H. F. Aliabadi. A Novel Multi-Fidelity Modelling-Based Framework for Reliability-Based Design Optimization of Composite Structures. Engineering with Computers. January 2020.

[31] Dassault Systèmes. Abaqus 6.13 Documentation, April 2013.

[32] United States Federal Aviation Administration and Battelle Memorial Institute. Columbus Laboratories. MMPDS-08: Metallic Materials Properties Development and Standardization Federal Aviation Administration, Virginia, United States, 2006.

[33] W. Ramberg and W. R. Osgood. Description of Stress-Strain Curves by Three Parameters. TN 902, NACA, National Advisory Committee for Aeronautics; Washington, DC, United States, July 1943.

[34] A. Shahbazian and Y. C. Wang. Calculating the global buckling resistance of thin-walled steel members with uniform and non-uniform elevated temperatures under axial compression. Thin-Walled Structures, 49:1415–1428, May 2011.

[35] D. Quinn et al. Stiffened Panel Stability Behavior and Performance Gains with Plate Prismatic Sub-Stiffening, Thin-Walled Structures 47 (2009). Pg.1457–1468

[36] S. Gholizadeh, A. Pirmoz, and R. Attarnejad. Assessment of Load Carrying Capacity of Castellated Steel Beams by Neural Networks. Journal of Constructional Steel Research, 67(5):770–779, 2011.

[37] S. Haykin. Neural Networks: A Comprehensive Foundation. Prentice Hall, 1999.

[38] K. Gurney. An Introduction to Neural Networks. Taylor & Francis, 2003.

[39] J. Feldman and R. Rojas. Neural Networks: A Systematic Introduction. Springer Berlin Heidelberg, 1996.

[40] A. Cankur. Development of an Artificial Neural Network Based Analysis Method for Skin-Stringer Structures. Master's Thesis, Middle East Technical University, Ankara, September 2017.

[41] H. M. Gomes and A. M. Awruch. Comparison of Response Surface and Neural Network with Other Methods for Structural Reliability Analysis. Structural Safety, 26(1):49–67, 2004.

[42] M.H. Beale, M.T. Hagan, and H.B. Demuth. Neural Network Toolbox: For Use with MATLAB; [User's Guide]. MathWorks, 1992.

[43] A. Krenker, A. Kos, and J. Bešter. Introduction to the Artificial Neural Networks. INTECH Open Access Publisher, 2011.

[44] M. Stein, "Large Sample Properties of Simulations using Latin Hypercube Sampling", American Statistical Association and the American Society for Quality Control, Technometrics, 1987.

[45] S. Kucherenko, D. Albrecht and A. Saltelli, Exploring multi-dimensional spaces: a Comparison of Latin Hypercube and Quasi Monte Carlo Sampling Techniques, May 2015.

[46] R. L. Iman, Latin Hypercube Sampling, Computer-Intensıve Statistical Methods Simple Random Sampling Stratified Designs, January 1999.

[47] R.C.Aydin, et. al. General Multi-Fidelity Framework for Training Artificial Neural Networks with Computational Models. Frontier in Materials. April 2019.

[48] N. Boely and R. M. Botez, Identification and Validation of a F/A-18 Model Using Neural Networks. In: AIAA Atmospheric Flight Mechanics Conference. Toronto, Ontario Canada, 2010

APPENDICES

A. Aluminum 7050-T7451 Material Properties (MMPDS-08)

Table 3.7.5.0(b$_1$). Design Mechanical and Physical Properties of 7050 Aluminum Alloy Plate

Specification	AMS 4050															
Form	Plate															
Temper	T7451															
Thickness, in.	0.250-1.500		1.501-2.000		2.001-3.000		3.001-4.000		4.001-5.000		5.001-6.000		6.001 -7.000		7.001 - 8.000	
Basis	A	B	A	B	A	B	A	B	A	B	A	B	A	B	A	B
Mechanical Properties:																
F_{tu}, ksi:																
L	74[a]	76	74	76	73[a]	75	72	74	71[a]	73	70[a]	72	69	72	68	71
LT	74	76	74[a]	76	73[a]	75	72	75	71[a]	74	70	73	69	72	68	71
ST	...	...	...	...	68	72	68[a]	71	67	70	66	69	66	68	65	67
F_{ty}, ksi:																
L	64[b]	67	64[b]	66	63[b]	66	62[b]	65	61[b]	65	60	63	59	62	58[b]	63
LT	64	66	64	66	63[b]	66	62	65	61	64	60	62	59	62	58	61
ST	...	...	...	...	59	61	57	60	57[b]	60	57	59	56	58	55[b]	58
F_{cy}, ksi:																
L	63	64	62	64	61	64	60	63	58	61	57	59	56	59	55	57
LT	66	68	67	69	66	69	65	68	64	67	63	66	60	63	59	62
ST	...	...	...	...	63	66	63	66	63	66	62	64	60	63	59	62
F_{su}, ksi																
L-S	43	44	44	45	43	45	44	45	43	45	43	45	44	46	44	46
T-S	42	43	43	44	43	44	43	45	43	45	43	45	44	46	44	46
S-L	...	...	...	...	...	...	...	...	...	...	...	...	...	...	...	...
F_{bru}[c], ksi:																
(e/D = 1.5)																
L	107	110	109	112	108	111	107	111	107	111	105	110	107	112	103	108
LT	109	112	111	114	110	113	109	113	108	113	107	112	109	114	107	112
ST	...	...	...	...	...	...	...	...	...	...	...	...	...	...	...	...
(e/D = 2.0)																
L	140	145	142	146	141	144	140	144	138	144	137	142	136	143	132	138
LT	140	144	142	146	141	145	141	145	139	145	138	144	139	146	137	143
ST	...	...	...	...	...	...	...	...	...	...	...	...	...	...	...	...
F_{bry}[c], ksi:																
(e/D = 1.5)																
L	86	89	89	92	89	93	90	94	90	95	91	94	84	89	83	87
LT	87	89	90	92	89	94	90	95	90	95	91	94	85	90	84	88
ST	...	...	...	...	...	...	...	...	...	...	...	...	...	...	...	...
(e/D = 2.0)																
L	101	104	104	107	104	109	104	109	105	110	105	108	99	105	98	102
LT	103	106	106	110	106	111	106	111	106	111	106	110	99	105	98	103
ST	...	...	...	...	...	...	...	...	...	...	...	...	...	...	...	...

Table 3.7.5.0(b$_1$). Design Mechanical and Physical Properties of 7050 Aluminum Alloy Plate (Continued)

Specification	AMS 4050															
Form	Plate															
Temper	T7451															
Thickness, in.	0.250-1.500		1.501-2.000		2.001-3.000		3.001-4.000		4.001-5.000		5.001-6.000		6.001 -7.000		7.001 - 8.000	
Basis	A	B	A	B	A	B	A	B	A	B	A	B	A	B	A	B
e, percent (S-Basis):																
L	10	...	10	...	9	...	9	...	9	...	8	...	7	...	6	...
LT	9	...	9	...	8	...	6	...	5	...	4	...	4	...	4	...
ST	...	...	...	...	3	...	3	...	3	...	3	...	3	...	3	...
E, 10^3 ksi	10.3															
E_c, 10^3 ksi	10.6															
G, 10^3 ksi	3.9															
μ	0.33															
Physical Properties:																
ω, lb/in.^{3}	0.102															
C, Btu/(lb)(°F)	0.23 (at 212°F)															
K, Btu/[(hr)(ft^2)(°F)/ft]	91 (at 77°F)															
α, 10^{-6} in./in./°F	12.8 (68°to 212°F)															

Figure A.1. Properties of 7050-T7451 Plate